Anti-inflammatory potential of Sesquiterpene Lactones

Subjects: Pharmacology & Pharmacy | Biochemistry & Molecular Biology

Contributor: Melanie Matos

Inflammation is a crucial and complex process that reestablishes the physiological state after a noxious stimulus. In pathological conditions the inflammatory state may persist, leading to chronic inflammation and causing tissue damage. Sesquiterpene lactones (SLs) are composed of a large and diverse group of highly bioactive plant secondary metabolites, characterized by a 15-carbon backbone structure. In recent years, the interest in SLs has risen due to their vast array of biological activities beneficial for human health. The anti-inflammatory potential of these compounds results from their ability to target and inhibit various key pro-inflammatory molecules enrolled in diverse inflammatory pathways, and prevent or reduce the inflammatory damage on tissues. Research on the anti-inflammatory mechanisms of SLs has thrived over the last years, and numerous compounds from diverse plants have been studied, using in silico, in vitro, and in vivo assays. Besides their anti-inflammatory potential, their cytotoxicity, structure–activity relationships, and pharmacokinetics have been investigated.

anti-inflammatory | bioactivity | sesquiterpene lactone-rich natural extracts | germacranolides | guaianolides | eudesmanolides | heliangolides | pseudoguainolides | inflammatory pathway | NF-κB | pro-inflammatory mediators

1. Sesquiterpene Lactones

Sesquiterpene lactones (SLs) are composed of a large and diverse group of phytochemicals found in numerous plant families, with the greatest number of compounds belonging to the *Asteraceae* family [1]. These molecules derive from two main precursors, isopentenyl diphosphate (IPP), and dimethylallyl diphosphate (DMAPP) [2][3]. These precursors can be generated in plants via either the mevalonate pathway, which occurs within the cytosol, or the 2-C-methyl-D-erythritol pathway, occurring in the chloroplasts [2][3]. IPP and DMAPP are converted into farnesyl diphosphate (FPP) by the enzyme farnesyl diphosphate synthase [4][5]. FPP is considered a common precursor for SLs, but can be further converted to sterols, triterpenes, or used for prenylationed of proteins. Its cyclization by germacrene A synthase into germacrene A is considered as the first step towards SL production [2]. Germacrene A is subsequently oxidized by a cytochrome P450 enzyme, germacrene A oxidase, into germacrene A acid. This molecule can be further modified to produce different subclasses of SLs, with the characteristic 15-carbon backbone structure [4][5][6] [7].

SLs are characterized by a 15-carbon backbone containing α,β-unsaturated carbonyl structures, such as a conserved α-methylene-γ-lactone (**Figure 1**). Numerous other modifications to the molecular structure are also known, including the presence of hydroxyls, esters, and epoxides [8][9]. There are over 5000 reported structures of SLs, divided into several skeletal subtypes, the main ones being germacranolides, guaianolides, eudesmanolides, heliangolides, and pseudoguaianolides (**Figure 2**) [1][10].

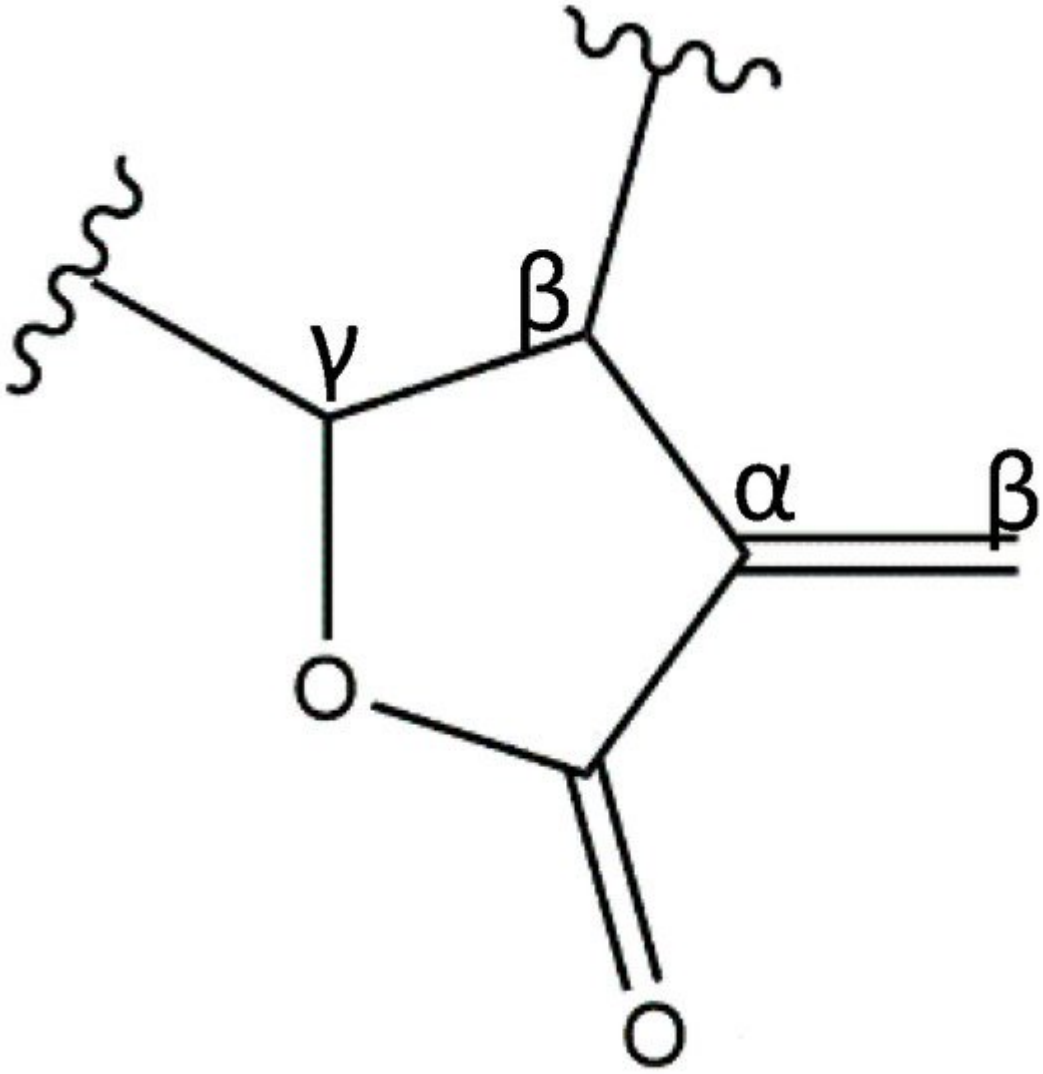

Figure 1. α-methylene-γ-lactone moiety core structure characteristic of SLs.

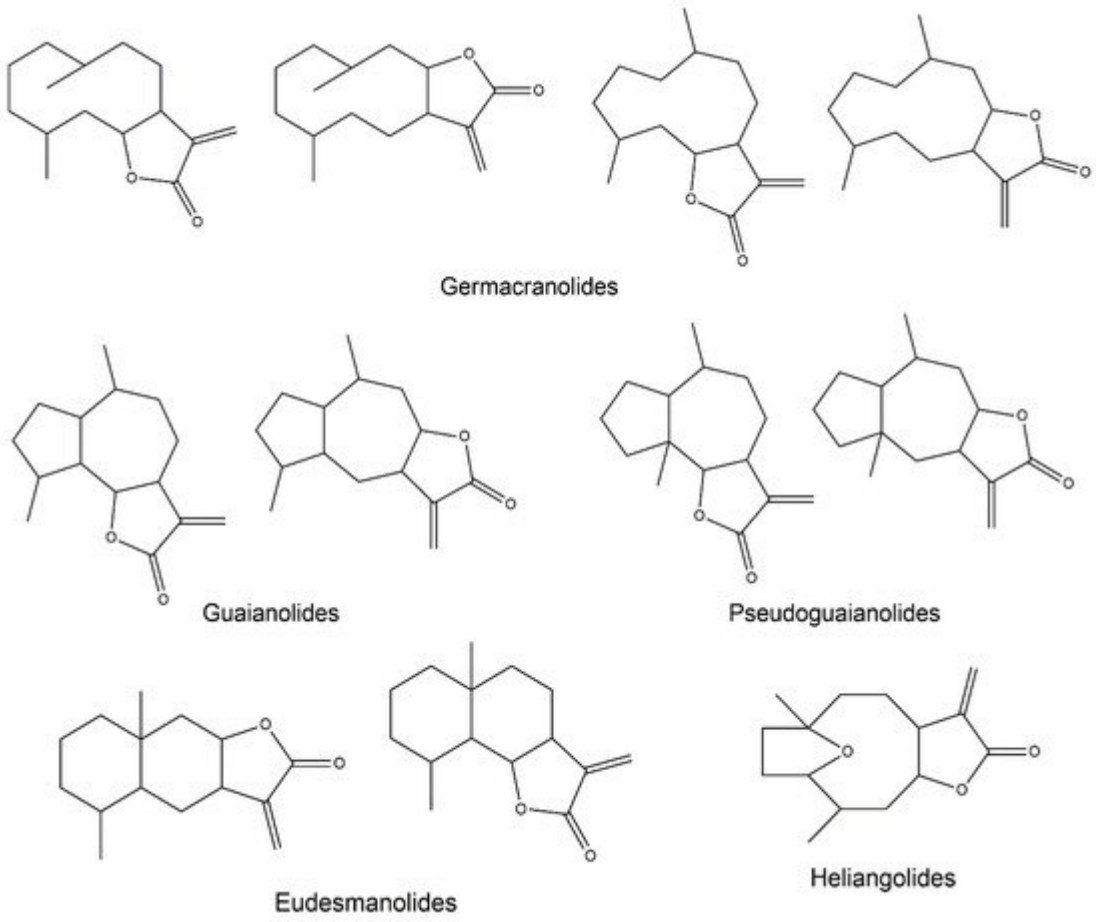

Figure 2. Structural backbone of the main SL subclasses.

In recent years, the interest in SLs has risen considerably due to their vast array of biological activities relevant to human health. This curiosity has led to many studies regarding the isolation of these compounds from natural sources, the development of complete or semi-synthesis procedures, and the evaluation of the pharmacological potential of SLs and their derivatives. Some of the many known activities reported for this class of compounds include anti-microbial, anti-fungal, anti-viral, anti-tumor, anti-malarial, anti-diabetic, analgesic, and anti-inflammatory activities [1][11]. There is a close relationship between the pharmacological potential of SLs and their respective ecological purposes, since their main goals in nature consist of anti-microbial and anti-herbivore endeavors, as well as the growth inhibition of competing plants [12].

The electrophilic α,β-unsaturated carbonyl moieties present in SLs, which react by Michael-type addition with biological nucleophiles, can explain the wide range of observed biological activities. In particular, sulfhydryl groups present in biomolecules, such as glutathione (GSH) or proteins with free cysteine groups, are major targets for alkylation by SLs (**Figure 3**) [8][10]. Consequently, the function of these biomolecules may become significantly impaired and lead to decreased activity in the case of enzymes, or disruption of the cellular redox balance through interference with the GSH metabolism, which ultimately promotes apoptosis [1]. Although covalent modifications are considered the lead mechanism of action carried out by most SLs, non-covalent interactions with specific molecules can also play a part in the bioactivity of these compounds [10].

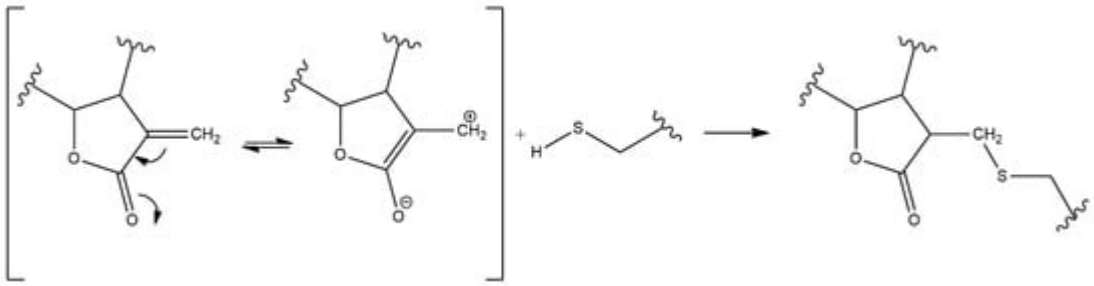

Figure 3. Michael reaction between an α-methylene-γ-lactone moiety and a sulfhydryl group.

Although the effects of SLs depend on varied factors, namely, the compound structure, the concentration used, and the organism assayed, SLs are generally considered highly toxic compounds, due to their somewhat unspecific mechanism of action. In fact, structural features responsible for therapeutic bioactivities are sometimes the ones responsible for toxic effects. Nonetheless, given their pronounced biological potential and “drug-like” physicochemical properties (based on Lipinski’s rule of five), SLs have been looked upon as very promising lead compounds.

2. Anti-Inflammatory Potential of Sesquiterpene Lactones

2.1. General Notes on Inflammation

Inflammation is a complex immune response that restores tissue homeostasis after a noxious stimulus, such as infection or tissue injury. It is a crucial process but can become detrimental when it occurs in excess due to its tissue-damaging potential since several types of unspecific effector molecules are released, causing collateral damage. In the case of transitory abnormal conditions, an acute inflammatory response successfully restores the system’s basal homeostatic setpoints after pathogen clearance or tissue repair. However, if the inflammatory trigger persists, the ongoing inflammatory state shifts the system to different setpoints, and acute inflammation may progress to chronic inflammation and, ultimately, disease [13][14]. Chronic inflammation is involved in ailments such as asthma, allergies, rheumatoid arthritis, multiple sclerosis, psoriasis, or inflammatory bowel diseases, and is known to be associated with a higher risk of cancer development [15].

Glucocorticoids and nonsteroidal anti-inflammatory drugs (NSAIDs) are the most common anti-inflammatory drugs. However, they present several adverse side effects after prolonged exposure. Thereby, the identification of novel compounds that can resolve inflammation without the adverse side effects caused by currently used anti-inflammatory therapies is of the utmost importance.

The different pathways by which SLs present their anti-inflammatory potential will be further discussed in the following sections of this review. Indeed, research on the anti-inflammatory mechanisms of action of pure SLs and SL-rich extracts has thrived over the last few years, with a vast number of publications resorting to in silico, in vitro, and in vivo models. This review aims to gather the most relevant results and insights concerning the anti-

inflammatory potential of SL-containing extracts and pure SLs, focusing on their effect on different inflammatory pathways.

2.2. SL-Containing Extracts

The rise of SLs as promising bioactive molecules is a consequence of the use of SL-rich plant extracts in traditional medicine for the treatment of various ailments over the centuries. Reports of the anti-inflammatory potential of natural extracts containing SLs can be found in many studies dedicated to different plant species from the *Asteraceae* family, which is characterized by having structurally diverse SLs [16]. Both in vitro and in vivo evidence indicates that this class of compounds can exert their effect on several inflammatory pathways (**Table 1**).

Table 1. Anti-inflammatory effects of SL-containing natural extracts in different in vitro and in vivo experimental models. The affected inflammatory pathways are described, as well as the experimental outcomes observed in each study, and the extract concentration range tested. ↓—decrease; ↑—increase.

Source	Main SLs		Model	Extract Concentration Range	Inflammatory Pathways	Consequences	References
Cichorium intybus L.	Dihydrolactucin, lactucin, deoxylactucin, jacquinelin and dihydrolactucopicrin	In vitro	RAW 264.7 murine macrophages + LPS	IC_{50} (µg/mL): 117 for COX-2; 39 for iNOS; 48 for TNF-α; 22 for IL-1β; 21 for NO	-	↓ COX-2, iNOS, TNF-α, IL-1β, NO	[17]
		In vivo	Paw edema model: Wistar rats + carrageenan (subcutaneous)	50–100 mg/kg (oral administration)	-	↓ paw volume (edema)	
			Arthritis model: Wistar rats + collagen (intravenous)	200 mg/kg (oral administration)	-		
Artemisia leucodes L.	Leukomisin and austricin	In vitro	RAW264.7 murine macrophages + LPS	2–100 µg/mL	-	↓ COX-2, iNOS, IL-1β, NO	[18]
			COX-1 and -2 enzymatic assay	45–225 µg/mL		↓ COX-2	
		In vivo	Paw edema model: Wistar rats + carrageenan (subcutaneous)	50–200 mg/kg (oral administration)		↓ paw edema	

Source	Main SLs		Model	Extract Concentration Range	Inflammatory Pathways	Consequences	References
			Chronic inflammation model: Wistar rats + cotton implant granuloma test	50 mg/kg (oral administration)		↓ granuloma and inflammatory cell infiltrate	
Artemisia khorassanica L.	Unspecified	In vitro	J774A.1 murine macrophages + LPS	10–100 µg/mL	↓ NF-κB	↓ COX-2, PGE_2, iNOS, NO, TNF-α and IL-1β	[19]
Artemisia sps (*A. kopetdaghensis, A. santolina, A. Sieberi, A. Fragrans, A. Absinthium, A. ciniformis*)	Saturated, unsaturated and unusual SLs	In vitro	J774A.1 murine macrophages + LPS	10–100 µg/mL	-	↓ COX-2, PGE_2, iNOS and NO	[20]
Eupatorium perfoliatum L.	Diguaiaperfolin (dimeric guaianolide) and Eupafolin (flavonoid)	In vitro	RAW264.7 murine macrophages + LPS	1–100 µg/mL	-	↓ NO, CSF-3, IL-6, IL-1α, IL-1β, TNF, Chemokine (C-C motif) ligand (CCL)-2, CCL22 and CXCL10	[21]
Xanthium spinosum L.	Ziniolide	In vitro	Rat polymorphonuclear leukocytes (PMNLs) + ionophore A23187 and Ca^{2+}	0–100 µg/mL	↓ NF-κB and arachidonic acid	↓ 5-LOX	[22]
			Human platelets + ionophore A23187	25–200 µg/mL		↓ COX-1 and 12-LOX; ↑ 15(S)-HETE	
			HeLa cells + Phorbol 12-myristate 13-acetate (PMA)	12.5–100 µg/mL		↓ NF-κB activation	
Arnica montana L.	Helenalin and dihydrohelenalin ester derivatives	In vitro	Jurkat T cells + TNF-α or PMA	0.5–10 µL/mL	↓ NF-κB and NFAT	↓ NF-κB and NFAT DNA-binding	[23]

Source	Main SLs		Model	Extract Concentration Range	Inflammatory Pathways	Consequences	References
			Human PBMCs from healthy donors + LPS	0.001–10 µL/mL		↓ TNF-α and IL-1β	
Centaurea L. species (*C. aphrodisea, C. athoa, C. hyalolepis, C. iberica, C. polyclada*)	SL fraction (athoin, 14-O-acetylathoin and methyl-14-O-acetylathoin-12-oate in C. *athoa*)	In vitro	SW1353 human chondrosarcoma cells + PMA	0–100 µg/mL	↓ NF-κB	↓ NF-κB activity	[24][25]
			RAW264.7 murine macrophages + LPS			↓ NO	
		In vivo	Paw edema model: Wistar rats + carrageenan (subcutaneous)	6.75–50 mg/kg (oral administration)		↓ edema	
Inula helenium L.	Alantolactone and isoalantolactone	In vitro	bEnd.3 mouse endothelial cells + TNF-α	0.6–2.4 µg/mL	↓ NF-κB and MAPKs	↓NF-κB inhibitor (IκB)-α, NF-κB p65, p38 and c-Jun N-terminal kinase (JNK) phosphorylation	[26]
			RAW264.7 murine macrophages + LPS			↓ IL-1, IL-6 and iNOS	
			Primary synovial fibroblasts from rheumatoid arthritis patients + TNF-α	50		↓ IL-1, MCP-1 and MMP-3	
		In vivo [17]	Adjuvant-induced mice arthritis model	12.5–50 mg/kg (oral administration)	[17]	↓ paw swelling	
			Collagen-induced mice arthritis model				
Arctium lappa L.	Onopordopicrin	In vivo [18]	Colitis model: Wistar rats + Trinitrobenzene Sulfonic Acid (TNBS) (enteral instillation)	25–50 mg/kg (oral administration)	-	↓ TNF-α and COX-2; ↓ histological damage; ↓ mucin layer loss; ↓ neutrophil infiltration [18]	[27]

elin, and (COX-2) mmatory ıg/mL) in ssion of e for the ylactucin ısing the ed in the d it was nd iNOS ombined lies, SL-

containing extracts presented anti-inflammatory effects comparable to those of known drugs. That is the case with oral administration of the chicory extract, which demonstrated a comparable effect to that of indomethacin in a carrageenan-induced rat paw edema model, by reducing the inflammation and paw volume [17]. The same extract displayed a prolonged effect in a collagen-induced arthritis model, by significantly reducing inflammation until 5 days after the end of the treatment [17]. In the case of *Artemisia leucodes*, oral administration of the extract itself was more effective than aspirin in reducing the swelling in a rat paw edema model, as well as reducing the immune cell infiltrate and granuloma formation in a cotton granuloma test (chronic inflammation challenge) [18]. This underlines that, in some cases, an extract containing several compounds may produce a more potent anti-inflammatory response than one pure compound.

Similarly, the treatment of LPS-induced J774A.1 macrophages with an SL-rich fraction from *Artemisia khorassanica* L. reduced nitric oxide (NO), TNF-α, IL-1β, as well as prostaglandin E_2 (PGE_2), which is one of the main products

Source	Main SLs		Model	Extract Concentration Range [19]	Inflammatory Pathways	Consequences	References
Vernonia scorpioides L.	Diacethylpiptocarphol and related hirsutinolides	In vivo	Acute ear edema model: Swiss mice + 12-O-tetradecanoylphorbol acetate (TPA) (topical)	0.003–1 mg (topical)	[18][19] ↓ NF-κB	↓ neutrophil infiltration, edema and epidermal proliferation	[20][38]
			Chronic ear edema model: Swiss mice + arachidonic acid (topical) or croton oil (topical)	1 mg (topical) [20]			

A dichloromethane extract from *Eupatorium perfoliatum* L. containing SLs was tested in RAW264.7 macrophages, and it was able to reduce both iNOS expression and NO production. The main compounds identified in the extract were isolated and investigated, revealing that the dimeric guaianolide diguaiaperfolin and the flavonoid eupafolin were the main active constituents. The extract also decreased the expression of several cytokines at both the gene and protein levels, namely the IL-1 and TNF families, as well as IL-6, which is generally produced as a response to stimulation by the previous two, and the colony-stimulating factor-3 (CSF-3), responsible for activating granulocytes. The authors suggested that the effect caused by the extract could have been in part due to eupafolin, a non-SL compound identified as one of the main active constituents of the extract [21].

Xanthium spinosum L. methanolic extract inhibited COX-1 and 12-lipoxygenase (12-LOX) enzymatic pathways in human platelets and increased the synthesis of the anti-inflammatory eicosanoid 15-Hydroxyeicosatetraenoic acid (15(S)-HETE), which is an inhibitor of phospholipase A_2 [22]. The extract also inhibited 5-lipoxygenase (5-LOX) in rat polymorphonuclear leukocytes (PMNLs), and a 5-LOX bioguided fractionation of the extract resulted in the isolation of the known 12,8-guaianolide ziniolide [22]. A 1 h pre-incubation with either the extract or isolated ziniolide was capable of inhibiting NF-κB signaling after a 7 h inflammatory stimulus, which may contribute to a more lasting anti-inflammatory effect. However, the more immediate inhibitory effects on eicosanoid biosynthesis, observed after a short incubation of only a few minutes, resulted from the direct interaction with the AA pathway enzymes rather than the mediation by NF-κB inhibition [22].

Extracts prepared from the Arbo and Spanish varieties of *Arnica montana* L., rich in helenalin and dihydrohelenalin esters, inhibited IL-1β and TNF-α release in peripheral blood mononuclear cells (PBMCs), as well as the deoxyribonucleic acid (DNA)-binding of the transcription factors NF-κB and the nuclear factor of activated T-cells (NFAT) in Jurkat cells, both of which are responsible for the transcription of pro-inflammatory genes [23]. The Arbo variety was shown to be more effective than the Spanish one, a result attributed to the fact that the main SLs present in the former were helenalin-derivatives, as opposed to the predominant dihydrohelenalin-derivatives in the latter [23]. These results underline the importance of the α-methylene-γ-lactone moiety in the bioactive potential of SLs. Besides the core structure of the SL, it was demonstrated in Jurkat T cells that the SL derivatives esterified with unsaturated acids, such as methacrylate or tiglinate, were more active than those esterified with saturated acids, such as acetate, a result that was confirmed in vivo when 11α,13-dihydrohelenalin methacrylate was shown to be more effective than 11α,13-dihydrohelenalin acetate in inhibiting the swelling in a mouse ear edema model [23]. It is also worth mentioning that preliminary studies carried out by the authors suggested that the mechanism of

NFAT inhibition is different from the one described for the known immunosuppressants tacrolimus (FK506) and cyclosporin [23], which highlights the potential of SLs as alternative anti-inflammatory leads to circumvent the side effects of currently used drugs.

In a study comprising extracts from different *Centaurea* species obtained with different solvents (*n*-hexane, chloroform, or methanol), chloroform extracts were the most effective in inhibiting NF-κB and iNOS, bioactivities that were attributed to the presence of SLs, which tend to be preferentially extracted by this solvent due to their hydrophobicity [24]. A chloroform extract from *C. athoa* was highlighted as the one with the most promising anti-inflammatory potential. The extract inhibited NF-κB activity in vitro in human chondrosarcoma cells, to the same extent as the pure germacranolide parthenolide, which was considered as the positive control [24]. Moreover, oral administration of this same extract to rats reduced the swelling in an in vivo paw edema model [24]. A follow-up study from the same group revealed athoin, 14-*O*-acetylathoin, and methyl-14-*O*-acetylathoin-12-oate to be the main SLs present in *C. athoa* [25].

Gao et al. [26] suggested the oral use of the *Inula helenium* L. extract, mainly composed of alantolactone and isoalantolactone, for the prevention and treatment of rheumatoid arthritis, after the promising results obtained in vitro and in vivo. In particular, the extract inhibited NF-κB and MAPKs activation in bEnd.3 mouse endothelial cells, and decreased the release of the pro-inflammatory mediator IL-1, the monocyte chemoattractant protein (MCP-1), and matrix metalloproteinase (MMP)-3 in primary synovial fibroblasts from patients, as well as IL-6 and iNOS in murine macrophages [26]. Additionally, in rats, oral administration of the extract improved rheumatoid arthritis symptoms in both the developing and the developed phases of the disease [26].

Oral administration of a fraction from *Arctium lappa* L. enriched in the germacranolide onopordopicrin decreased colitis-associated histological damage in rats and prevented mucin layer loss, which is a common feature of inflammatory bowel diseases (IBD) responsible for a defective barrier function. Additionally, neutrophil infiltration was reduced, as well as the production of TNF-α and COX-2, whereas COX-1 was not affected [27].

The concentrations upon which SL molecules are pharmacologically active are not well defined, and although SLs are described as poorly bioavailable [29], the aforementioned in vivo reports show that, in many cases, orally administered SLs are pharmacologically active against inflammation. These conclusions highlight the anti-inflammatory potential of orally administered SLs, thereby reinforcing the importance of studying their pharmacokinetic (ADME—Absorption, Distribution, Metabolism, Excretion) profile of these molecules. On the other hand, a topical application was also shown to be effective in both acute and chronic inflammatory processes when a *Vernonia scorpioides* L. extract, containing diacethylpiptocarphol and related hirsutinolides, was used to treat dermatitis and psoriasis in mice [28]. The extract reduced edema, neutrophil infiltration, and epidermal hyperproliferation, possibly through the inhibition of the chemotactic cytokine IL-8 and NF-κB activity, and its effectiveness was comparable to that of dexamethasone [28].

Although many natural extracts containing SLs show promising anti-inflammatory potential (**Table 1**), one must keep in mind that extracts may be complex mixtures containing several compounds from different classes that

might interact with each other producing synergistic or antagonistic effects. Therefore, while extracts may be useful as adjuvant therapies, the major potential is provided by individual compounds that might be considered leads for the pharmaceutical industry. For this reason, to validate their anti-inflammatory applicability, SLs must be isolated from their natural sources and their effect must be studied further. In the following section, the relevant studies based on pure SLs are gathered and are divided by SL subclasses.

2.3. Germacranolides

2.3.1. Parthenolide

Germacranolides are undoubtedly the most extensively studied class of SLs due to the well-known pharmacological potential of parthenolide. It was first isolated from the medicinal plant feverfew (*Tanacetum parthenium* L.), which inspired the scientific community to further explore other germacranolides. Parthenolide (**Figure 4**) works as an anti-inflammatory and anti-cancer agent, and both bioactivities are mainly driven by its capacity to interfere with the NF-κB pathway, since this transcription factor controls the proliferative, the anti-apoptotic, as well as the pro-inflammatory genes [30]. Given that several signaling pathways rely on NF-κB, the anti-inflammatory success of parthenolide can be assessed by its effect on numerous indirect targets [30]. As an example, the treatment of LPS/interferon (IFN)-γ-stimulated rat aortic smooth muscle cells with parthenolide prevented NO release and iNOS gene expression, via the stabilization of the IκBα/NF-κB complex by inhibiting the degradation of the former and the nuclear translocation of the latter [31].

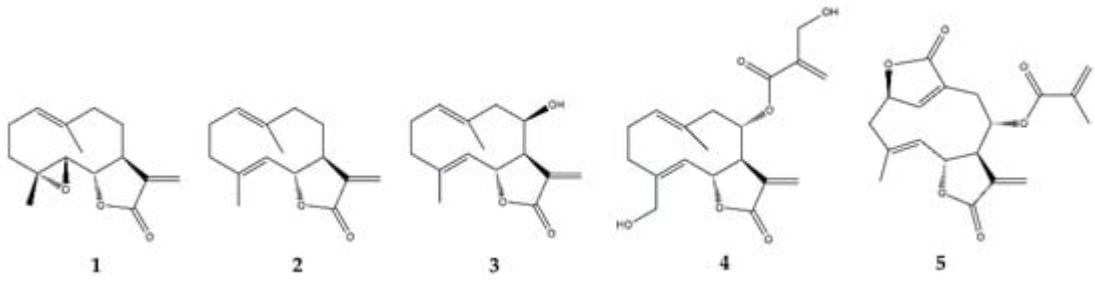

Figure 4. Structures of addressed germacranolides. **1**—Parthenolide; **2**—Costunolide; **3**—Eupatolide; **4**—Onopordopicrin; **5**—Deoxyelepantopin.

Parthenolide appears to have the potential to reduce brain inflammation, and its lipophilic character favors blood–brain barrier (BBB) permeability, factors that make this germacranolide a promising agent to treat glioblastomas and offer explanations for the anti-migraine efficacy of orally administered *Tanacetum parthenium* L., a major known source of parthenolide [32][33]. For instance, parthenolide dose-dependently decreased IL-6 and TNF-α release in LPS-stimulated BV-2 microglia [32], as well as rat primary neuro-glial cells [33], probably because of its strong ability to reduce NF-κB nuclear translocation and the subsequent transcription of pro-inflammatory genes. In rats, an injection of a low dosage of parthenolide before LPS stimulation attenuates oxidative stress, brain inflammation, and fever [33]. These effects could be explained by the decreased activation of NF-κB and nuclear respiratory factor (Nrf)-1 (a reactive oxygen species (ROS)-induced transcription factor), and by the reduced expression of COX-2 (critical in the generation of the known fever mediator PGE_2) in the hypothalamus [33].

In another research study, parthenolide inhibited IL-4, and to a lesser extent, IL-2 and IFN-γ expression in Jurkat T cells activated by phorbol 12-myristate 13-acetate (PMA)/ionomycin or anti-CD3/CD28 antibodies, by blocking the NF-κB pathway. These results were confirmed in primary human T lymphocytes from both healthy and allergic donors when 2.5 μM parthenolide could completely suppress the IL-4 protein levels, while higher doses were required for the same effect to be achieved for IL-2 and IFN-γ. Although all three cytokines are NF-κB-regulated genes, their different responses to parthenolide raises the possibility of using this compound to treat allergic diseases, which are mainly mediated by the preferential differentiation of Th2 over Th1 lymphocytes, directed by IL-4 stimulation [34]. In another study, parthenolide inhibited the activation of T-cells in whole blood by hindering the expression of IL-2, a mediator of lymphocyte proliferation and activation [35]. In this case, the SL acted in a step prior to the differentiation into CD4 or CD8 T-cells, possibly by interfering with the activation of either the activator protein 1 (AP-1), NF-κB, NFAT or octamer transcription factor-1 (Oct-1), all of which are transcription factors that control IL-2 expression [35].

Li et al. [36] hypothesized that the inhibition of the Toll-like receptor 4 (TLR4) signaling pathway could reduce LPS-induced inflammation, since the binding of LPS to this receptor leads to MAPKs activation and the nuclear translocation of NF-κB to induce pro-inflammatory cytokine release. Indeed, parthenolide was able to inhibit the phosphorylation of MAPKs, IκBα, and p65, and counteract the upregulation of several pro-inflammatory cytokines, after LPS stimulation in monocytes. Because these inflammatory events can reflect TLR4 activation, and since parthenolide inhibits the LPS-induced upregulation of TLR4, the authors stated that the anti-inflammatory effects of this SL are due to its ability to inhibit the TLR4 signaling pathway. Nevertheless, although parthenolide may operate partly through TLR4-mediated signaling, its direct effect on the MAPK and NF-κB pathways must not be overlooked.

In a rat model, the intraperitoneal administration of either parthenolide or enhydrin, another germacranolide, significantly attenuated the paw edema and hyperalgesia caused by a carrageenan injection [37]. Such results make these germacranolides potential alternatives to NSAIDs. However, the SL derivative 11β,13-dihydroparthenolide was not able to reverse carrageenan-induced inflammatory nociception, possibly due to the lack of the α-methylene-γ-lactone group [37].

2.3.2. Costunolide

Costunolide (**Figure 4**), another well-described germacranolide, was first isolated from *Saussurea lappa* L. and can modulate several intracellular signaling pathways involved in inflammation. Costunolide's mode of action is in many ways similar to that of parthenolide. In particular, the timing of the treatment for either parthenolide or costunolide to obtain an anti-inflammatory effect was proven to be critical, given that both SLs were more effective when applied before the inflammatory stimuli in a pre-treatment approach, rather than in a simultaneous incubation with the inflammatory insult [33][38]. Specifically, parthenolide can diminish an LPS-induced fever, inflammation, and oxidative stress in rats when injected before LPS stimulation but not when administered simultaneously with LPS [33]. In turn, costunolide was more effective in preventing IL-6 and TNF-α release in murine macrophages when the cells were pre-incubated with the SL before being elicited with LPS, as opposed to what was seen in the case of a

simultaneous incubation with both costunolide and LPS [38]. These observations make sense, since the bioactivity of SLs is driven by a modulation of the transcription factors' signaling pathways, which needs some time to occur. In addition, the importance of the presence of an α-methylene-γ-lactone group in costunolide also became evident when an α-methylene-γ-butyrolactone structure induced heme oxygenase-1 (HO-1) expression as well as Nrf-2 activity and nuclear translocation to the same extent as costunolide in RAW264.7 macrophages, while the α-methyl-γ-butyrolactone and γ-butyrolactone structures did not (**Figure 5**) [38]. The induction of the antioxidant enzyme HO-1 via the Nrf-2 pathway explained the ability of costunolide to decrease TNF-α and IL-6 [38].

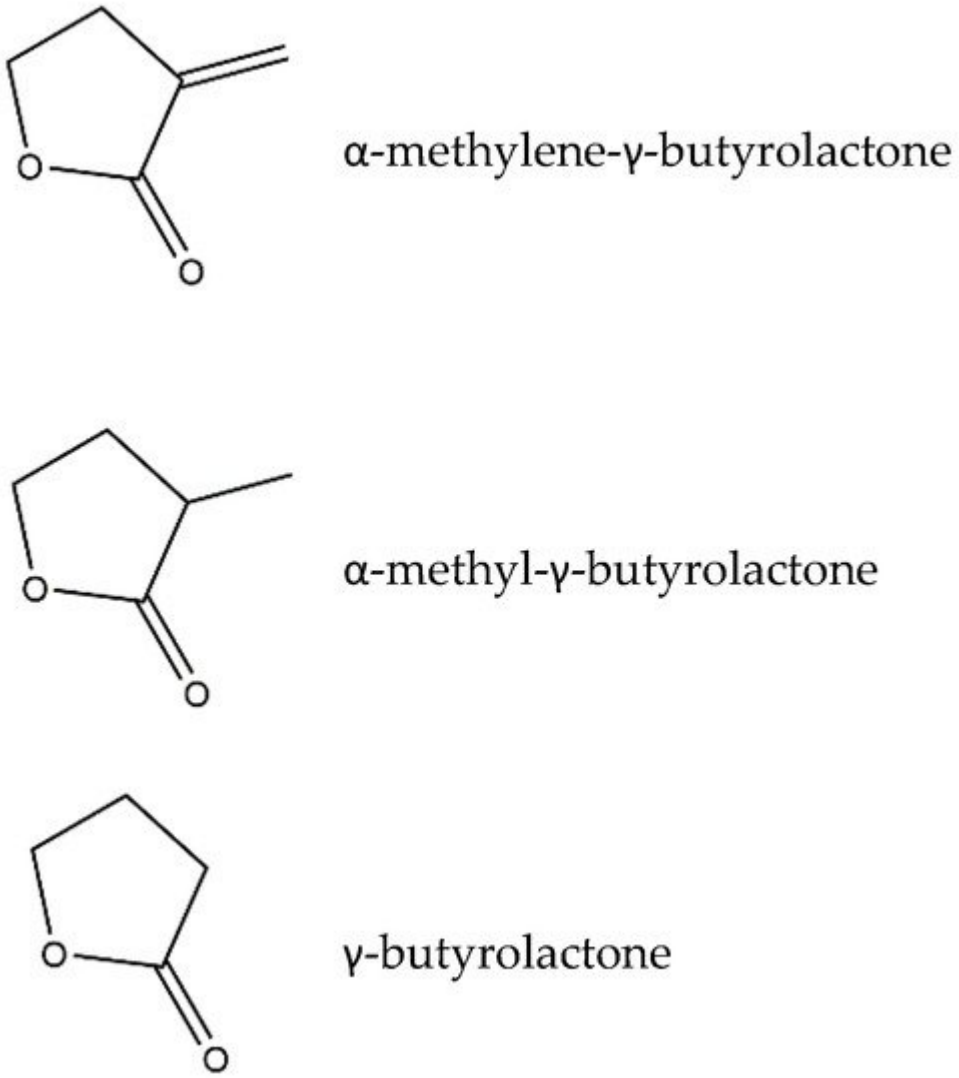

Figure 5. Structures of α-methylene-γ-butyrolactone, α-methyl-γ-butyrolactone, and γ-butyrolactone.

Although the NF-κB pathway is one of the main targets of parthenolide and costunolide, other transcription factors have also been addressed as targets. In HepG2 hepatocytes, parthenolide inhibited the IL-6-induced expression of acute-phase protein genes, which are intimately related to inflammatory responses [39]. Parthenolide blocks the phosphorylation of signal transducers and the activators of transcription proteins (STATs), in particular STAT3, probably through the inactivation of the Janus kinases (JAKs) by conjugation with their thiol groups. Consequently, the STAT3 dimerization required for the nuclear translocation of the transcription complex does not take place [39].

Butturini et al. [40] drew similar conclusions concerning costunolide when it prevented the IL-6-elicited activation and the DNA-binding of STAT3 in the human monocytic cell line THP-1. These observations were due to the inhibition of the JAKs phosphorylation as well as the disturbance of the intracellular GSH levels, which in turn led to the glutathionylation of STAT3, thus inhibiting its phosphorylation. Once again, the reduced form of costunolide, lacking the α,β-unsaturated carbonyl, failed to inhibit the activation of STAT3 [40].

In another study comprising both costunolide and its derivative dihydrocostunolide, the α-methylene-γ-lactone proved its importance in the bioactivity of the SL structure once more. Costunolide was proposed for the treatment of psoriasis, as it is able to block the pro-inflammatory effects of IFN-γ and IL-22 in primary human keratinocytes through the inhibition of STAT1 and STAT3 activation. The compound also prevented epidermal hyperproliferation caused by an apoptosis-resistant phenotype [41]. In this case, the pro-oxidant effect of costunolide, caused by conjugation with GSH, was explored as the key aspect for activating the anti-proliferative and pro-apoptotic pathways that are crucial in counteracting the psoriatic phenotype [41].

AP-1 is another transcription factor upon which costunolide exerts its anti-inflammatory effect by inhibiting its DNA-binding activity as well the MAPKs signaling pathway that mediates its activation [42].

In IL-1β-elicited primary rat chondrocytes, costunolide prevented the expression of cytokines, iNOS, COX-2, and matrix metalloproteinases (MMPs), while upregulating collagen II and the transcription factor SRY-box transcrition factor (SOX)-9 (crucial for chondrocyte proliferation and differentiation). Such results were a consequence of the suppression of the NF-κB and Wnt/β-catenin pathways, that are both involved in bone metabolism and reconstruction [43]. These results were complemented by an in vivo attenuation of cartilage degeneration in rat joints, and costunolide was proposed as a promising agent to treat osteoarthritis [43].

An effect of costunolide against inflammatory angiogenesis, which is related to tumor growth and metastasis, was demonstrated in mice [44]. In addition to the attenuation of fibrovascular tissue (hemoglobin content and collagen deposition), along with reduced macrophage and neutrophil recruitment, the compound decreased inflammatory, angiogenic, and fibrogenic mediators, including the vascular endothelial growth factor (VEGF) and the transforming growth factor (TGF)-β [44].

2.3.3. Other Germacranolides

Research interest in SLs is evolving as the biological relevance of this class of compounds is growing, and underexplored germacranolides are emerging as promising novel anti-inflammatory agents. These compounds act in several pathways leading to the activation of different transcription factors that ultimately result in the expression of inflammation-related proteins.

Eupatolide (**Figure 4**) is a germacranolide that inhibits the activation of both the MAPKs and protein kinase B (Akt) pathways, as well as the phosphorylation of IκBα and p65, thus suppressing the NF-κB and AP-1 transcription factors, which in turn leads to the decreased expression of iNOS and COX-2 along with the resulting NO and PGE_2 [45]. These outcomes might be a consequence of the eupatolide-induced proteasomal degradation of the tumor

necrosis factor receptor (TNFR)-associated factor 6 (TRAF6), which mediates the activation of signaling pathways, including NF-κB and MAPKs [45].

Onopordopicrin (**Figure 4**), isolated from *Onopordum Illyricum* L., revealed its potential as a potent inhibitor of NF-κB and STAT3 while promoting the activation of Nrf2, an agent of antioxidant defense [46].

In addition to the interference with the transcription factors involved in inflammation, advanced research on different mechanisms of action is also being conducted. Recently, deoxyelephantopin (**Figure 4**), another germacranolide, has been implicated in a novel strategy to treat inflammatory diseases [47]. This compound decreased macrophage activation and prevented sepsis-mediated death in mice by attenuating aerobic glycolysis at the transcription and protein expression levels of several key glycolytic enzymes [47]. The connection to inflammation lies in the fact that activated immune cells reprogram their energy metabolism from oxidative phosphorylation to aerobic glycolysis, a phenomenon equivalent to the Warburg effect of tumor cells.

Deoxyelephantopin dose-dependently inhibited NO in the LPS-induced murine macrophage cell line RAW 264.7. This decrease was due to the downregulation of the iNOS mRNA and protein levels in macrophages. The compound was also able to decrease the amounts of COX-2 at the mRNA and protein levels while reducing the production of TNF-α and IL-6 back to basal levels [48]. These results were consistent with NF-κB inhibition and the authors confirmed that deoxyelephantopin could prevent the nuclear translocation of the p65 subunit by suppressing the phosphorylation and degradation of IκB, which maintains the nuclear transcription factor inactive in the cytosol, ultimately inhibiting the production of pro-inflammatory cytokines [48]. Deoxyelephantopin was also able to suppress, in vivo, the activation of the IL6/STAT3 pathway and JNK1 and JNK2 in mice liver cells, inhibiting the production of pro-inflammatory cytokines. Moreover, the protein levels of the suppressor of cytokine signaling (SOCS)-3, which is a key component of IL-6 negative regulation, were decreased in deoxyelephantopin treatment of an LPS/D-Galactosamine-induced hepatic inflammation model in mice. Deoxyelephantopin could also attenuate the levels of TNF-α and IL-6 in mice serum, as well as effectively reduce the activity of the iNOS and COX-2 proteins in the hepatic inflammation mice model [48].

2.4. Guaianolides

Guaianolides recently isolated from *Ormenis mixta* L. and characterized as 2,3-epoxy-1,4,10-trihydroxyguaian-12,6α-olide diastereoisomers, revealed an anti-inflammatory potential through the inhibition of NO release and COX-2 expression in murine macrophages treated with LPS [49].

Dehydrocostuslactone (**Figure 6**) exerts its anti-inflammatory effects through the inhibition of several inflammatory pathways. The treatment of THP-1 cells with dehydrocostuslactone showed its ability to inhibit the activation of the IL-6/STAT3 pathway. Moreover, it suggested that dehydrocostuslactone was able to interact directly with the cellular glutathione content. This interaction created intracellular oxidative stress, leading to the inhibition of STAT3 tyrosine-phosphorylation in IL-6-induced cells, resulting in a downregulation of the expression of genes involved in inflammatory processes, in particular, MCP-1, the C-X-C motif chemokine ligand 10 (CXCL10), and the intracellular adhesion molecule-1 (ICAM-1), with an EC_{50} of 10 µM [40][41]. The ability of dehydrocostuslactone to suppress the

tyrosine-phosphorylation of STAT3 suggests that this compound may interfere with the functions of upstream JAK kinases, associated with a portion of the IL-6 receptor. Additionally, dehydrocostuslactone also interfered with IL-22/STAT3 in keratinocytes, resulting in the downregulation of inflammatory genes. The most sensitive genes to the action of this SL were those transcriptionally regulated by STAT3 and whose regulation is driven by the extracellular signal-regulated kinase (ERK) 1 [41].

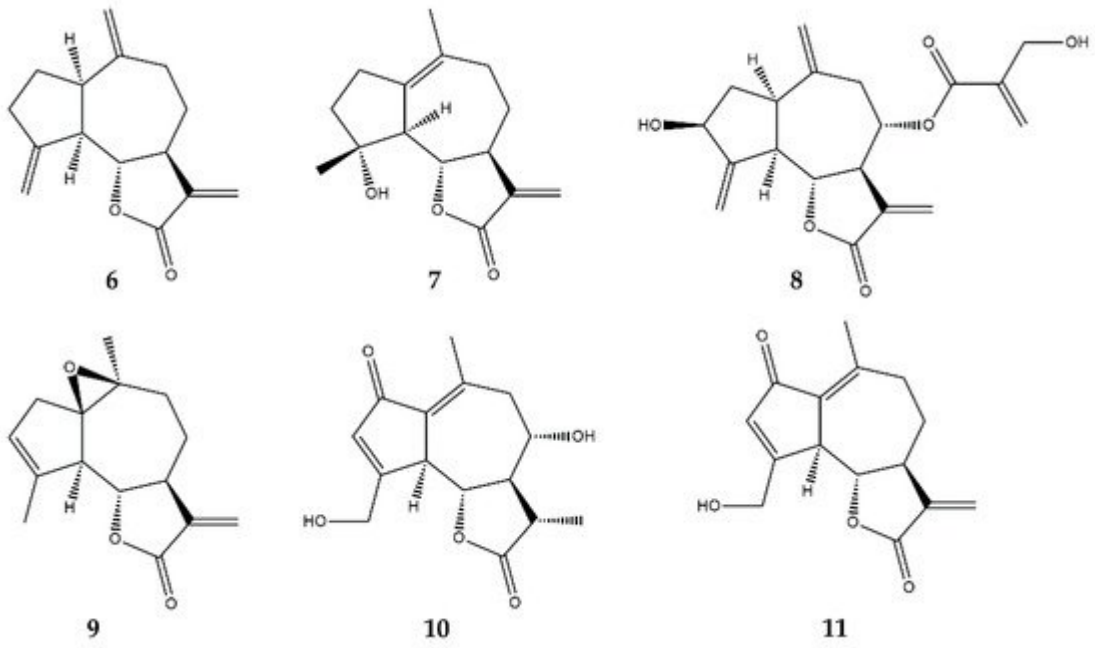

Figure 6. Structures of addressed guaianolides. **6**—Dehydrocostuslactone; **7**—Micheliolide; **8**—Cynaropicrin; **9**—Arglabin; **10**—11β,13-dihydrolactucin; **11**—8-deoxylactucin.

In a dextran sulfate sodium (DSS)-induced colitis in mice, dehydrocostuslactone (20 mg/kg/day, orally administrated) reduced the quantity of inflammatory cytokines, such as TNF-α, IL-1β, MCP-1, myeloperoxidase (MPO), superoxidase dismutase (SOD), IL-6, IL-17, and IL-23, and once again downregulated the IL-6/STAT3 inflammatory signaling pathway, thus alleviating the colorectal damage caused by DSS [40][41][50]. The decreased activity of this pathway is related to the further downregulation of other inflammatory mediators, such as iNOS and COX-2 [50].

In a different study, dehydrocostuslactone (20 μM) inhibited both the NF-κB pathway and the interferon regulatory factor 3 (IRF3) in LPS-stimulated murine macrophages RAW 264.7 [51], with both transcription factors being regulated upstream by the activation of the Toll-like receptors myeloid differentiation primary response 88 (MyD88) and Toll-interleukin-1 receptor domain-containing adapter- inducing interferon-β (TRIF)-dependent signaling pathways. By suppressing these receptors, dehydrocostuslactone downregulated NF-κB and IRF3, consequently preventing the expression of their target genes including COX-2, INF-β, and the interferon gamma-induced protein-10 (IP-10). Moreover, the treatment of LPS-challenged macrophages with dehydrocostuslactone leads to the suppression of IκBα degradation, strengthening the NF-κB inhibition [51].

Micheliolide (**Figure 6**), another guaianolide, may pose a therapeutic benefit for the treatment of neurodegenerative disorders via the inhibition of LPS-induced iNOS and COX-2 protein expression in BV2 microglial cells [52]. The compound (10 μM) also demonstrated the ability to attenuate, at the transcriptional level, the expression of multiple pro-inflammatory mediators, namely, TNF-α, IL-6, IL-1β, COX-2, and iNOS, all the genes of which are regulated by the activation of the NF-κB transcription factor and the Akt pathway [52]. The authors verified that micheliolide could block the NF-κB p65 subunit nuclear translocation, maintaining the transcription factor inactive in the cytosol [52][53]. In the same study, micheliolide was shown to exert anti-inflammatory activity by inhibiting the activation of MAPKs, including JNK, p38, and ERK1/2, and phosphatidyl inositol 3-kinase (PI3K)/Akt. Both of these pathways culminate in the activation of NF-κB, which underlines the ability of this compound to inhibit this transcription factor and further downregulate the NF-κB-dependent inflammation players [52].

In a different study, micheliolide proved its ability to decrease inflammatory cytokine production in murine macrophages RAW 264.7, human dendritic cells, and monocytes. The authors demonstrated that micheliolide inhibited the LPS-induced activation of NF-κB and the PI3K/Akt pathway [54].

In vivo studies also demonstrated that pre-treatment with micheliolide, diluted in the drinking water of mice, five days before inflammatory stimuli with DSS, was able to reduce neutrophil and lymphocyte infiltration, attenuating the severity of colitis and the inflammatory damage to the colon tissue. The authors further verified that the administration of micheliolide strongly inhibited IL-6, TNF-α, and IL-1β expression in a murine model of DSS-induced colitis [53].

In an acute peritonitis mouse model, micheliolide (20 mg/kg, intradermal injection) was able to reduce the secretion of IL-6, TNF-α, IL-1β, and MCP-1, resulting in a decreased inflammatory state [54][55]. In a collagen-induced arthritis mouse model, micheliolide, administered intraperitoneally, reduced paw swelling and suppressed the degeneration of articular cartilage, whilst also decreasing the levels of several inflammatory mediators such as the tissue inhibitor of metalloproteinases (TIMP)-1, macrophage colony-stimulating factor (M-CSF), ICAM-1, and INF-γ, thereby reducing the proliferation, adhesion, and infiltration of leukocytes into the affected area [55].

The guaianolide cynaropicrin (**Figure 6**) possesses anti-inflammatory properties, strongly inhibiting TNF-α release from LPS-stimulated murine RAW 264.7 macrophages, and differentiated human macrophages (U937 cells). Aside from TNF-α inhibition, the compound was also effective in reducing the release of NO from RAW 264.7 macrophages stimulated with LPS and IFN-γ, in a dose-dependent manner [56]. Cynaropicrin also suppressed the proliferation of $CD4^+$, $CD8^+$ T-, and B- lymphocytes [56].

Arglabin (**Figure 6**) was described as able to attenuate the overexpression of inflammatory mediators with a decrease in the mRNA levels of NF-κB-regulated genes, such as COX-2, iNOS, and IL-1β in peritoneal mouse macrophages [57]. In vivo, arglabin (2.5 ng/g, intraperitoneal injection, twice daily for thirteen days) inhibited the nucleotide-binding oligomeriztion domain (NOD)-like receptor family pyrin domain-containing 3 (NLRP3) inflammasome activity and significantly reduced the production of the cytokines IL-1α, IL-1β, and IL-18, leading to a reduction in the atherosclerotic lesions in apolipoprotein E (apoE)-deficient mice with an EC_{50} of 10 nM [57].

11β,13-dihydrolactucin (**Figure 6**) has been revealed as possessing anti-inflammatory potential by reducing the activity of the calcineurin/calcineurin-responsive zinc finger-1 (Crz1) pathway, which is the yeast orthologue of the human calcineurin/NFAT pathway. Calcineurin is highly conserved between eukaryotes making this an optimal model for screening potential anti-inflammatory compounds [58]. 11β,13-dihydrolactucin reduced the activation of the pathway with an IC_{50} of 2.35 μM. Further analysis demonstrated that the compound inhibited the nuclear translocation of Crz1, which remained inactive in the cytosol, in the presence of inflammatory stimuli [58].

8-deoxylactucin (**Figure 6**) has been described as the most effective SL in a chicory extract. The compound exerts its anti-inflammatory activity by inhibiting COX-2 protein and further downregulating PGE_2 in human colorectal cancer cells HT29 [59].

2.5. Eudesmanolides

Alantolactone and isoalantolactone (**Figure 7**) isolated from *Inula helenium* inhibited the TNF-α-induced activation of the NF-κB and MAPK pathways in mouse endothelial b.End3 cells, suppressed the expression of MMP-3, MCP-1, and IL-1 in synovial fibroblasts, and decreased the expression of IL-1, IL-6, and iNOS in murine macrophages RAW 264.7 [26]. In vivo, alantolactone (orally administered, 50 mg/kg) could also alleviate the arthritic severity and paw swelling in either the developing or the developed phases of adjuvant and collagen-induced arthritis in a mice model [26].

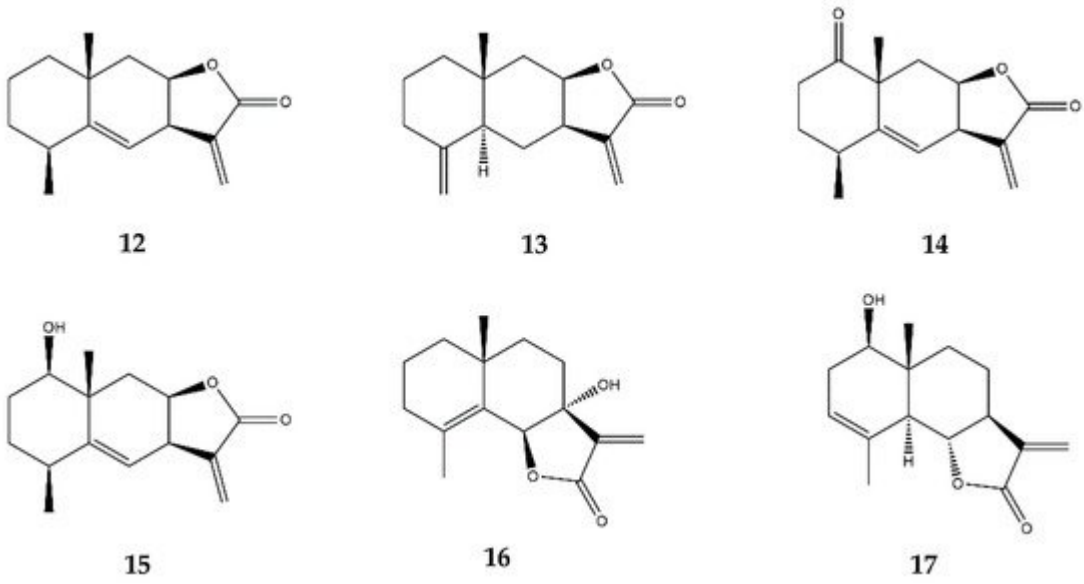

Figure 7. Structures of addressed eudesmanolides. **12**—Alantolactone; **13**—Isoalantolactone; **14**—JEUD-38; **15**—1β-hydroxyalantolactone; **16**—7-hydroxyfrullanolide; **17**—Santamarin.

In another study, alantolactone was able to inhibit iNOS and COX-2 at both the mRNA and the protein levels. Furthermore, alantolactone reduced the production of pro-inflammatory markers such as NO, PGE_2, and TNF-α [60]. Regarding the NF-κB pathway, alantolactone not only inhibited the DNA-binding of the NF-κB p65 subunit, but also suppressed IκB kinase (IKK) phosphorylation, resulting in the blockage of the IκB degradation and the subsequent activation of the NF-κB transcriptional factor [60]. The authors concluded that these effects might occur

due to inhibition of the MyD88 and the Toll-interleukin-1 receptor domain-containing adapter protein (TIRAP), an upstream signaling molecule involved in IKK and MAPK activation, in LPS-stimulated macrophages [60].

In an in vitro intestinal inflammation model, alantolactone inhibited NF-κB nuclear translocation and dose-dependently activated the human pregnane X receptor (hPXR), a key regulator gene in IBD pathogenesis [61]. hPXR inhibits NF-κB-driven gene expression. However, NF-κB can also regulate hPXR-driven gene expression. The authors demonstrated that alantolactone directly interacts with the hPXR, thus enhancing the inhibition of the NF-κB pathway, which suggests that the anti-inflammatory effect of alantolactone could be partially driven by the activation of hPXR [61]. In an in vivo model of intestinal inflammation, the oral administration of alantolactone (50 mg/kg) significantly ameliorated the clinical symptoms of DSS-induced colitis in mice by lowering the release of pro-inflammatory mediators such as iNOS, ICAM-1, COX-2, TNF-α, INF-γ, and IL-6 to basal levels [61].

Isoalantolactone (**Figure 7**), a variant of alantolactone, similarly to its parental compound was also found to inhibit, in vitro, the TNF-α-stimulated activation of the NF-κB and MAPKs pathways in b.End3 cells, suppress the expression of MMP-3, MCP-1, and IL-1 in TNF-α-stimulated synovial fibroblasts, and reduce IL-1 and IL-6 production in LPS-stimulated murine RAW 264.7 macrophages [26].

1β-hydroxyalantolactone (**Figure 7**) peculiarly demonstrates its anti-inflammatory effects by inhibiting the ubiquitin-conjugating enzyme H5 (UbcH5) during TNF-α-induced NF-κB activation. This enzyme mediates the ubiquitination of several important signaling proteins upstream of IKK, resulting in a non-phosphorylated IKK that is in turn unable to degrade IκB, thereby preventing the further activation of NF-κB and ultimately suppressing the downstream pro-inflammatory gene expression [62].

JEUD-38 (**Figure 7**) is a recently discovered SL from *Inula japonica* L., a plant from the Asteraceae family, which inhibited the nuclear translocation of p65 by impeding IκBα phosphorylation and degradation in murine RAW264.7 macrophages [63]. In addition, JEUD-38 inhibited the LPS-stimulated phosphorylation of MAPKs, including ERK1, ERK2, JNK, and p38 kinases, further strengthening its inhibitory effects on NF-κB suppression [63].

7-hydroxyfrullanolide (**Figure 7**) suppressed the LPS-induced NF-κB-related transcripts in human PMBCs and in freshly collected synovial cells from rheumatoid arthritis patients, by inhibiting the nuclear translocation of NF-κB through the inhibition of IKK phosphorylation in THP-1 cells [64]. Since NF-κB regulates the transcription of adhesion molecules, the authors further explored the expression of ICAM-1, vascular cell adhesion molecule (VCAM)-1, and E-selectin in LPS-stimulated endothelial cells, concluding that treatment with 7-hydroxyfrullanolide suppressed their production and also inhibited monocyte adhesion [64]. 7-hydroxyfrullanolide was also tested in different animal inflammation models, in which oral administration dose-dependently diminished the induced and spontaneous production of TNF-α along with IL-6 in a BALB/c ear edema model and in DSS-induced colitis in mice [65]. Administration of 7-hydroxyfrullanolide also attenuated rectal bleeding and colonic edema, and diminished the shortening of the colon, as was verified by histological images [65].

Santamarin (**Figure 7**) inhibited the activation of the iNOS and COX-2 proteins, consequently reducing their respective products, namely NO and PGE_2 in LPS-stimulated RAW 264.7 cells and murine peritoneal macrophages [66]. Santamarin also reduced TNF-α and IL-1β production by suppressing the phosphorylation and degradation of IκBα, and by blocking the nuclear translocation of p65 in response to LPS in RAW 264.7 macrophages [66]. Additionally, both the mRNA and protein levels of the anti-inflammatory protein HO-1 were upregulated in the presence of Santamarin [66]. HO-1 is primarily regulated at the transcriptional level, and it may be induced by various agents, including the Nfr2 transcription factor. The effects of Santamarin on NO, PGE_2, and TNF-α production were partially reversed by the usage of an HO-1 inhibitor, suggesting that part of the anti-inflammatory effect demonstrated by Santamarin is related to the induction of HO-1 [66].

2.6. Heliangolides

In vitro assays demonstrated that lychnopholide (**Figure 8**) inhibited NO production in J774A.1 macrophages stimulated by INF-γ and LPS, and increased the production of IL-10, an anti-inflammatory cytokine [67]. In vivo, lychnopholide reduced a carrageenan-induced paw edema when administered topically in ointment formulation at a concentration of 1% [67].

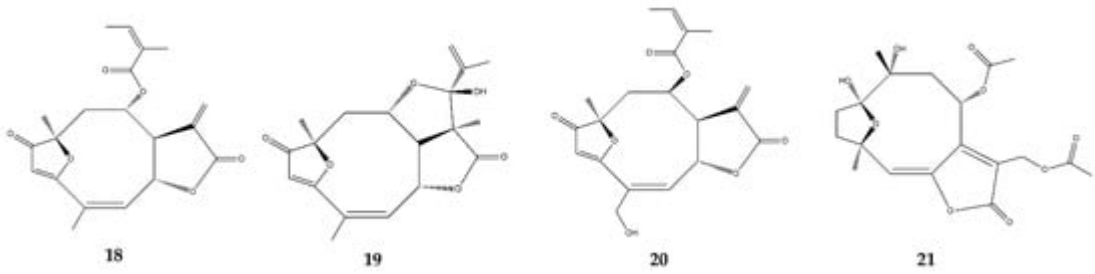

Figure 8. Structures of addressed heliangolides. **18**—Lychnopholide; **19**—Eremantholide C; **20**—Budlein A; **21**—Diacethylpiptocarphol.

Eremantholide C (**Figure 8**) was able to reduce TNF-α release while increasing IL-10 production in J774A.1 macrophages [67]. In vivo, eremantholide reduced the carrageenan-induced paw edema, possibly due to TNF-α inhibition and the induction of IL-10 production when applied topically in ointment formulation at a concentration of 1% [67].

Budlein A (**Figure 8**), a furanoheliangolide, possesses anti-inflammatory activities related to the inhibition of pro-inflammatory cytokines and neutrophil recruitment. In vitro, budlein A reduced the NF-κB activity in murine macrophages RAW 264.7 [68]. Treatment with budlein A decreased neutrophil recruitment in models of innate immune response and inhibited the LPS-induced expression of adhesion molecules such as E-selectin, ICAM-1, and VCAM-1, all of which are correlated with NF-κB inhibition [68]. The authors also showed that budlein A reduces lymphocyte proliferation and the release of IL-2 and INF-γ. The effect of budlein A was also evaluated in antigen-induced arthritis in mice, in which it dose-dependently inhibited IL-33, TNF-α, IL-1β, and COX-2 mRNA expression [68]. In another study, budlein A inhibited carrageenan-induced neutrophil migration to the peritoneal cavity, neutrophil migration to the paw skin tissue, paw edema, and mechanical hypernociception [69]. Moreover, the

treatment inhibited the mechanical hypernociception induced by TNF-α and IL-1β but not the hypernociception caused by PGE_2 or dopamine [69]. In a similar study, budlein A was tested as a therapeutic agent against gout arthritis in a murine model, in which it prevented NF-κB activation by inhibiting TNF-α production, and attenuated neutrophil recruitment [70]. An in vitro analysis demonstrated that, in addition to TNF-α inhibition, budlein A reduced the production/maturation of IL-1β, suggesting that it may not only inhibit the NF-κB pathway but also interfere with the assembly of inflammasome NLRP3 in macrophages [70].

The intraperitoneal injection of diacethylpiptocarphol (**Figure 8**), a heliangolide isolated from *Vernonia scorpioides* L., in a DSS-induced colitis mouse model significantly decreased immune cell infiltration, tissue damage, and TNF-α release, while enhancing the production of TGF-β, which is involved in tissue remodeling. This newly isolated compound displayed results identical to those of parthenolide and the anti-inflammatory drug dexamethasone [71].

2.7. Pseudoguaianolides

Helenalin (**Figure 9**) is a known potent anti-inflammatory compound that can inhibit NF-κB activation in T- and B-lymphocytes, as well as in epithelial cells [72]. Whilst helenalin cannot prevent IκBα degradation nor NF-κB nuclear translocation, the compound can downregulate the pro-inflammatory NF-κB-driven gene expression by preventing the DNA-binding of the NF-κB p65 subunit since it modifies the active p65 by reacting with its free cysteines through Michael-type addition, thereby irreversibly alkylating its structure [72][73].

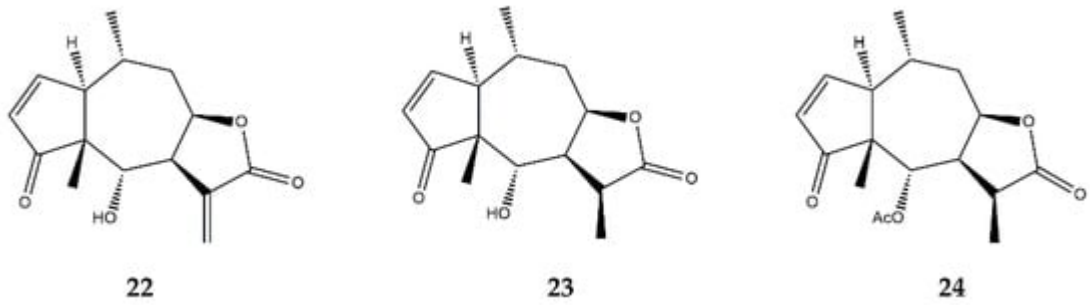

Figure 9. Structures of the addressed pseudoguaianolides: **22**—helenalin; **23**—11α,13-dihydrohelenalin; **24**—11α,13-dihydrohelenalin acetate.

Helenalin also demonstrates immunosuppressive effects in THP-1 cells, by decreasing cytokine release, namely the granulocyte-macrophage colony-stimulating factor (GM-CSF), IL-1α, IL-19, IL-23, and MCP-3. Since IL-19 plays a role in promoting the release of IL-6 and TNF-α, its suppression by helenalin is an important anti-inflammatory strategy [74][75]. The capacity of helenalin to inhibit the DNA-binding of the p65 subunit has been correlated with an increase in cellular death triggered by the mitochondrial pathway of apoptosis in CD4+ T-cells, which is a relevant anti-inflammatory effect [74][76]. T-cells that survive the exposure to helenalin undergo proliferation inhibition by the induction of G2/M cell cycle arrest [74]. Helenalin was also able to suppress the nuclear translocation of NFAT in activated $CD4^+$ T-cells, by decreasing the production of IL-2 in such lymphocytes [23][74].

11α,13-dihydrohelenalin (**Figure 9**) demonstrated the ability to inhibit DNA-binding as well as NF-κB activation, and although its variant 11α,13-dihydrohelenalin acetate was unable to prevent the DNA-binding of NF-κB, it significantly affected MAPKs, a result not verified for the parent compound [77]. Besides the NF-κB pathway and immune cell proliferation inhibition, helenalin and 11α,13-dihydrohelenalin acetate also display anti-inflammatory effects in the arachidonic acid pathway [78]. Helenalin and, to a lesser extent, 11α,13-dihydrohelenalin acetate, demonstrated the ability to inhibit both leukotriene C_4 synthase and 5-LOX in a concentration-dependent manner [78].

2.8. Other SL Subclasses

Vlasouliolides isolated from *Vladimiria souliei* L., consisting of rare SL dimeric structures with 32 carbons, presented an anti-inflammatory effect by inhibiting the phosphorylation of the NF-κB subunit p65 and preventing NO production in LPS-elicited murine macrophages [79].

It has also been described that artemisinin (**Figure 10**), a renowned SL due to its action against *Plasmodium falciparum* and therefore used in the treatment of malaria, significantly decreases the adhesion of monocytes to TNF-α-stimulated human umbilical vein endothelial cells (HUVECs), in a dose-dependent manner. The compound was also found to suppress the mRNA and protein levels of ICAM-1 and VCAM-1, leading to an attenuation of monocyte adhesion to HUVECs, which could be explained by the inhibition of the NF-κB signaling pathway [80]. Indeed, treatment with artemisinin also significantly increased the cytosolic levels of IκBα, the protein that maintains NF-κB in its inactive state, thus downregulating the expression of pro-inflammatory genes in the TNF-α-stimulated HUVECs [80]. Moreover, this SL was also found to inhibit the nuclear translocation of the activated p65 subunit of NF-κB and inhibit the ERK1 and ERK2 members of the MAPKs [80].

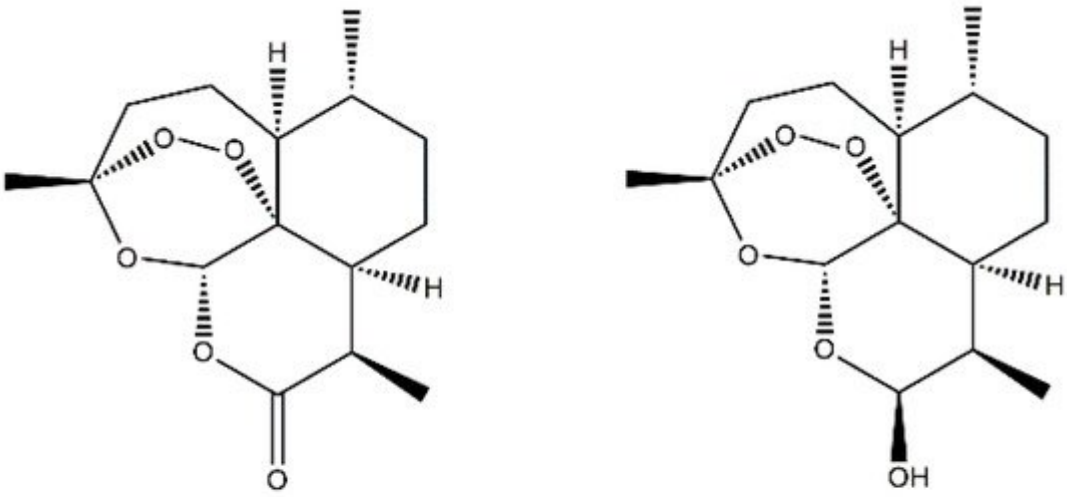

Figure 10. Structures of **25**—artemisinin and **26**—dihydroartemisinin.

Dihydroartemisinin (**Figure 10**) is a semi-synthetic derivate of artemisinin and has been described as having anti-inflammatory effects in murine RAW 264.7 macrophages with a dose-dependent decrease in the PMA-induced COX-2 expression and subsequent PGE_2 production [81]. These observations could be a result of dihydroartemisinin's inhibiting effects on the NF-κB, AP-1, and C/EBP pathways. Similar to the parent compound artemisinin, dihydroartemisinin also affected the MAPKs, inhibiting the activity of JNK, ERK1, ERK2, and p38 kinases [81].

A study conducted with 17 natural SLs belonging to the germacranolide, guaianolide, pseudoguaianolide, and eudesmanolide subclasses revealed that the bioactivities of these compounds are not always mediated by α,β-unsaturated carbonyl alkylation. In fact, the inhibition of isolated human neutrophil elastase, a protease implicated in the pathogenesis of several inflammatory diseases, was achieved by non-covalent interaction with the catalytic site, requiring the specific structural features of SLs such as a carbonyl group surrounded by hydroxy groups at a certain distance. Nonetheless, human neutrophil elastase was not considered a direct target for SLs, since most compounds require a high concentration to accomplish the inhibition of the enzyme [82].

Another set of varied SLs, including germacranolides, pseudoguaianolides, eudesmanolides, and heliangolides, was shown to effectively inhibit the activation of T-cells in whole blood samples, a probable consequence of the decreased expression of IL-2, a mediator of lymphocyte proliferation [35]. Interestingly, SLs presenting with only one α,β-unsaturated carbonyl moiety (monofunctional) were more effective than those with two of these functional groups (bifunctional) [35]. A reasonable explanation for this is the fact that the latter are more reactive and tend to bind to unspecific targets, such as albumin, thereby rendering them unavailable to react with the desired target. Less reactive SLs preferentially bind with targets for which they have the highest affinity rather than being trapped with matrix proteins.

The described anti-inflammatory outcomes of isolated SLs in the abovementioned models are summarized in **Table 2**.

Table 2. Anti-inflammatory effects of SLs belonging to the different SL subclasses in varied in vitro and in vivo experimental models. The affected inflammatory pathways are described, as well as the experimental outcomes observed in each study. ↓—decrease; ↑—increase.

SL Subclass	Compound Name (ID Number)		Model	Compound Concentration Ranges Tested	Inflammatory Pathways	Consequences	References
Germacranolides	Parthenolide (1)	In vitro	Rat aortic smooth muscle cells + LPS/IFN-γ	3–30 μM	↓ NF-κB	↓ iNOS and NO release	[31]
		In vitro	BV2 mouse microglia + LPS	5 μM	↓ NF-κB	↓ IL-6 and TNF-α	[32]
		In	Rat primary neural-	403 μM	↓ NF-κB, NF-IL6, Nrf-1 and	↓ IL-6 and TNF-α	[33]

SL Subclass	Compound Name (ID Number)		Model	Compound Concentration Ranges Tested	Inflammatory Pathways	Consequences	References
		vitro	glial cells + LPS		PGC1α		
		In vivo	Wistar rats + LPS (intraperitoneal injection)	1 mg/kg (intraperitoneal injection)		↓ IL-6 and TNF-α in plasma; ↓ COX-2, NF-IL6, SOCS3, IκBα and Tribbles pseudokinase 1 (Trib1) in hypothalamus; ↓ fever	
		In vitro	Jurkat T cells and primary peripheral human T cells + PMA/ionomycin or anti-CD3/CD28	1.25–5 μM	↓ NF-κB and AP-1	↓ IL-4, IL-2 and IFN-γ	[34]
		In vitro	Primary peripheral human T cells + PMA/ionomycin or anti-CD3/CD28	10–500 μM	-	↓ IL-2; ↓ T-lymphocyte activation	[35]
		In vitro	Human THP-1 monocytes + LPS	0.75–12 μM	↓ NF-κB and MAPKs	↓ IL-6, TNF-α, IL-1β, IL-8, IL-18 and NO; ↓ iNOS, TLR4 and TRAF6	[36]
		In vitro	Human primary monocytes + LPS				
		In vivo	Hindpaw edema model: Holtzman rats + carrageenan (subcutaneous injection)	5–20 mg/kg (intraperitoneal injection)	-	↓ Hyperalgesia and edema	[37]
		In vitro	HepG2 human hepatocytes + IL-6, oncostatin M or leukemia inhibitory factor	5 μM	↓ STAT3 and JAKs	↓ STAT3 phosphorylation, dimerization and activity	[39]
	Costunolide (2)	In vitro	Human THP-1 monocytes + IL-6	6–25 μM	↓ IL-6/STAT3 and JAKs	↓ MCP-1, CXCL10, ICAM-1; ↓ STAT3 phosphorylation	[40]

SL Subclass	Compound Name (ID Number)		Model	Compound Concentration Ranges Tested	Inflammatory Pathways	Consequences	References
						and DNA-binding activity; ↓ Intracellular GSH	
		In vitro	RAW264.7 murine macrophages + LPS	0.1–1 μM	↑ Nrf-2; ↓ NF-κB	↑ HO-1; ↓ IL-6 and TNF-α	[38]
		In vitro	Human keratinocytes from healthy donors + IL-22, IFN-γ or TNF-α	12.5 μM	↓ STAT3 and STAT1	↓ Intracellular GSH; ↓ CCL2, CXCL10, ICAM-1 and SOCS3; ↑ Epidermal growth factor receptor (EGFR) and Erk1/2	[41]
		In vitro	RAW264.7 murine macrophages + LPS	0.1–3 μM	↓ AP-1 and MAPKs	↓ IL-1β	[42]
		In vitro	Primary rat chondrocytes + IL-1β	2–6 μM	↓ NF-κB and Wnt/β-catenin; ↑ SOX-9	↓ MMP-3, MMP-9, MMP-13, iNOS, COX-2 and IL-6; ↑ collagen II	[43]
		In vivo	Sprague-Dawley rats (surgically induced osteoarthritis model)	6 μM (intra-articular injection)		attenuation of cartilage degeneration	
		In vivo	Angiogenesis model: Swiss albino mice + polyester-polyurethane sponge implants	5–20 mg/kg (cannula)	-	↓ Angiogenesis, macrophage and neutrophil accumulation, and collagen deposition; ↓ IL-1β, IL-6, IL-17, TNF-α, TGF-β; ↑ IL-10	[44]
	Eupatolide (3)	In vitro	RAW264.7 murine macrophages + LPS	0.1–10 μM	↓ NF-κB, AP-1, MAPKs, Akt	↓ COX-2, PGE_2, iNOS, NO and TRAF6	[45]
			Human embryonic kidney (HEK)-293			↑ proteossomal degradation of	

SL Subclass	Compound Name (ID Number)		Model	Compound Concentration Ranges Tested	Inflammatory Pathways	Consequences	References
			cells + LPS			TRAF6	
	Onopordopicrin (4)		NIH-3T3 cell line + TNF-α	IC_{50} (μM): 8.6 for NF-κB; 15.3 for STAT3; EC_{50} (μM): 2.2 for Nrf-2	↓ NF-κB and STAT3; ↑ Nrf-2	↓ NF-κB activity	[46]
		In vitro	HeLa cell line + IFN-γ			↓ STAT3 activity	
			HaCaT keratinocytes			↑ Nrf-2 activity	
	Deoxyelephantopin (5)	In vitro	RAW264.7 murine macrophages + LPS	2.5–10 μM	-	↓ high mobility group box (HMGB) 1, pyruvate kinase M2 (PKM2), glucose transporter 1 (GLUT1), lactate dehydrogenase A (LDHA) and phosphoinositide-dependent kinase 1 (PDK1) and IL-1β	[47]
		In vivo	C57BL/6J mice + LPS (intraperitoneal injection)	10 mg/kg (intraperitoneal injection)	-	↓ endotoxic shock and sepsis	
Guaianolides	Dehydrocostuslactone (6)	In vitro	THP-1 human cells + IL-6	6–25 μM	↓ IL-6/STAT3 and JAKs	↓ MCP-1, CXCL10, ICAM-1; ↓ STAT3 phosphorylation and DNA-binding activity; ↓ Intracellular GSH	[40]
		In vitro	Human keratinocytes from healthy donors + IL-22, IFN-γ or TNF-α	12.5 μM	↓ STAT3 and STAT1	↓ Intracellular GSH; ↓ CCL2, CXCL10, ICAM-1 and SOCS3; ↑ EGFR and Erk1/2	[41]
		In vivo	Colitis model: BALB/c mice + Dextran sulfate	10–20 mg/kg	↓ IL-6/STAT3	↓ TNF-α, IL-1β, MPO, SOD, IL-6, IL-17, IL-23, COX-2, iNOS	[50]

SL Subclass	Compound Name (ID Number)		Model	Compound Concentration Ranges Tested	Inflammatory Pathways	Consequences	References
			sodium (DSS) (oral administration)				
		In vitro	RAW 264.7 macrophages + LPS	10–20 μM	↓ MyD88/TRIF; ↓ NF-κB; ↓ IRF-3	↓ COX-2, INF-β, IP-10	[51]
		In vitro	BV2 microglia cells + LPS	1–10 μM	↓ NF-κB; ↓ PI3K/Akt ↓ MAPKs	↓ TNF-α, IL-6, IL-1β, COX-2, iNOS	[52]
	Micheliolide (7)	In vitro	RAW 264.7 macrophages + LPS	1–10 μM	↓ NF-κB	↓ IL-6, TNF-α, IL-1β	[53]
		In vitro	RAW264.7 macrophages + LPS	0–10 μM	↓ NF-κB; ↓ PI3K/Akt	↓ IL-6, TNF-α, MCP-1, INF-β and IL-1β	[54]
			Human dendritic cells and monocytes + LPS			↓ IL-6, TNF-α, MCP-1, INF-β	
		In vivo	Arthritis model: DBA/1 mice + collagen (intradermal injection)	30 mg/kg (intraperitoneal injection)	-	↓ TIMP-1, M-CSF, ICAM-1, INF-γ	[55]
	Cynaropicrin (8)	In vitro	RAW 264.7 macrophages + LPS	0–35 μM	-	↓ TNF-α and NO	[56]
			Human macrophages U937 + LPS				
			Primary splenocytes from mice + concanavalin A, phytohemagglutinin and LPS			↓ lymphocyte proliferation	
	Arglabin (9)	In vitro	Peritoneal macrophages from $ApoE_2$.Ki mice +	50 nM	↓ NF-κB; ↓ NLRP3	↓ IL-1α, IL-1β, IL-18	[57]

SL Subclass	Compound Name (ID Number)		Model	Compound Concentration Ranges Tested	Inflammatory Pathways	Consequences	References
			LPS and cholesterol crystals				
	11β,13-dihydrolactucin (10)	In vitro	Yeast *S. cerevisiae* + $MnCl_2$	0.36–18 μM	↓ Calcineurin-Crz1 (NFAT)	↓ NFAT nuclear translocation and transcriptional activity	[58]
	8-deoxylactucin (11)	In vitro	Human colon-cancer cells HT29 + TNF-α	115 μM	↓ NF-κB	↓ PGE_2	[59]
Eudesmanolides			bEnd.3 mouse endothelial cells + TNF-α			↓ IκBα, NF-κB p65, p38 and JNK phosphorylation	
		In vitro	RAW264.7 murine macrophages + LPS;	2.6–10.3 μM	↓ NF-κB and MAPKs	↓ IL-1, IL-6 and iNOS	[26]
	Alantolactone (12)		Primary synovial fibroblasts from rheumatoid arthritis patients + TNF-α			↓ IL-1, MCP-1 and MMP-3	
		In vitro	RAW 264.7 macrophages + LPS	1.25–10 μM	↓ NF-κB; ↓ MyD88	↓ iNOS, COX-2, TNF-α	[60]
		In vivo	Colitis model: C57BL/6 mice + DSS (oral administration)	50 mg/kg (oral administration)	↓ NF-κB; ↑ hPXR	↓ iNOS, ICAM-1, COX-2, TNF-α, IFN-γ, IL-6	[61]
	Isoalantolactone (13)		bEnd.3 mouse endothelial cells + TNF-α			↓ IκBα, NF-κB p65, p38 and JNK phosphorylation	
		In vitro	RAW264.7 murine macrophages + LPS	2.6–10.3 μM	↓ NF-κB and MAPKs	↓ IL-1, IL-6 and iNOS	[26]
			Primary synovial fibroblasts from rheumatoid arthritis patients + TNF-α			↓ IL-1, MCP-1 and MMP-3	
		In	293T cells + TNF-α	2.5–10 μM	↓ NF-κB and MAPKs	↓ UbcH5	[62]

SL Subclass	Compound Name (ID Number)		Model	Compound Concentration Ranges Tested	Inflammatory Pathways	Consequences	References
		vitro					
		In vivo	Hepatitis model: BALB/c mice + TNF-α and D-galactosamine (D-GalN) (intraperitoneal injection)	10 mg/kg (intraperitoneal injection)		↓ serum alanine aminotransferase (ALT); ↓ hepatocyte damage; ↓ IL-6, MCP-1, ICAM-1 and VCAM-1	
	JEUD-38 (14)	In vitro	RAW 264.7 macrophages + LPS	2.5–10 μM	↓ NF-κB and MAPKs	↓ iNOS	[63]
	7-hydroxyfrullanolide (16)	In vitro	THP-1 cell + LPS	0.3–100 μM	↓ NF-κB	↓ NF-κB activation and nuclear translocation	[64]
			HUVECs + LPS			↓ ICAM-1, VCAM-1, E-selectin ↓ Monocyte adhesion	
			PBMCs + LPS			↓ NF-κB-related gene expression	
			PBMCs + LPS				[65]
		In vitro	Primary human synovial tissue cells	0.3–100 μM	-	↓ IL-6 and TNF-α	
		In vivo	Colitis model: BALB/c mice + DSS (oral administration)	75 mg/kg (oral administration)	-	↓ TNF-α and IL-6; ↓ Colonic edema; ↓ Shortening of the colon; ↓ hemoglobin and rectal bleeding; ↓ neutrophil infiltration	
			Paw edema model: Wistar rats + carrageenan (subcutaneous injection)	100 mg/kg	-	↓ paw edema	
			Arthritis model: DBA/1J mice +	25–75 mg/kg (oral	-	↓ joint deformities and bone	

glandular trichomes of feverfew (Tanacetum parthenium L. Schulz Bip.). Phytochemistry 2011, 72, 1739–1750.

6. Amrehn, E.; Aschenbrenner, A.-K.; Heller, A.; Spring, O. Localization of sesquiterpene lactone biosynthesis in cells of capitate glandular trichomes of Helianthus annuus (Asteraceae). Protoplasma 2016, 253, 447–455.
7. Hussien, T.; Mohamed, T.; Elshamy, A.; Moustafa, M.; El-Seedi, H.; Pare, P.; Hegazy, M.-E. Guaianolide Sesquiterpene Lactones from Centaurothamnus maximus. Molecules 2021, 26, 2055.
8. Merfort, I. Perspectives on Sesquiterpene Lactones in Inflammation and Cancer. Curr. Drug Targets 2011, 12, 1560–1573.

SL Subclass	Compound Name (ID Number)		Model	Compound Concentration Ranges Tested	Inflammatory Pathways	Consequences	References
			collagen (intradermal injection)	administration)		destruction	
Heliangolides	Santamarin (17)	In vitro	RAW264.7 macrophages + LPS	5–40 μM	↓ NF-κB; ↑ Nfr2	↓ COX-2 and iNOS; ↓ TNF-α, IL-1β ↑ HO-1	[66]
			Murine peritoneal macrophages + LPS			↓ COX-2 and iNOS; ↓ TNF-α, IL-1β	
	Lychnopholide (18)	In vitro	J774A.1 macrophages + INF-γ and LPS	0.0125–0.2 μM	-	↑ IL-10; ↓ NO	[67]
	Eremantholide (19)		J774A.1 macrophages + INF-γ and LPS	0.625–10 μM	-	↑ IL-10; ↓ TNF-α	
	Budlein A (20)	In vitro	RAW264.7 + TNF-α or IL-1β	2.7×10^{4}–26.7 μM		↓ NF-κB activity	
		In vivo	Arthritis model: C57BL/6 mice + methylated bovine serum albumin (intra-articular injection)	1–10 mg/kg (oral administration)	↓ NF-κB	↓ edema; ↓ neutrophil and leukocyte infiltration; ↓ proteoglycan degradation; ↓ IL-33, TNF-α, IL-1β, COX-2	[68]
		In vivo	Paw edema model: Swiss mice + carrageenan (subcutaneous injection)	1–10 mg/kg	-	↓ TNF-α, IL-1β; ↓ edema, and neutrophil infiltration; ↓ mechanical hypernocecipetion	[69]
		In vivo	Gout arthritis model: Swiss mice + monosodium urate crystals (intra-articular injection)	1–10 mg/kg (oral administration)	↓ NF-κB; ↓ NLRP3 inflammasome	↓ TNF-α and IL-1β; ↓ neutrophil recruitment; ↓ edema and mechanical hypersensitivity	[70]

19. Emami, S.A.; Rabe, S.Z.T.; Iranshahi, M.; Ahi, A.; Mahmoudi, M. Sesquiterpene lactone fraction fromArtemisia khorassanicainhibits inducible nitric oxide synthase and cyclooxygenase-2 expression through the inactivation of NF-κB. Immunopharmacol. Immunotoxicol. 2010, 32, 688–695.
20. Zamani, S.; Emami, S.A.; Iranshahi, M.; Rabe, S.Z.T.; Mahmoudi, M. Sesquiterpene fractions of Artemisia plants as potent inhibitors of inducible nitric oxide synthase and cyclooxygenase-2 expression. Iran. J. Basic Med. Sci. 2019, 22, 774–780.
21. Maas, M.; Deters, A.M.; Hensel, A. Anti-inflammatory activity of Eupatorium perfoliatum L. extracts, eupafolin, and dimeric guaianolide via iNOS inhibitory activity and modulation of inflammation-related cytokines and chemokines. J. Ethnopharmacol. 2011, 137, 371–381.

SL Subclass	Compound Name (ID Number)		Model	Compound Concentration Ranges Tested	Inflammatory Pathways	Consequences	References
Bioactivity s		In vitro	Bone marrow derived macrophages (BMDMs) + LPS and monosodium urate crystals	2.7–26.7 mM		↓ TNF-α and IL-1β	
	Diacethylpiptocarphol (21)	In vivo	Colitis model: BALB/c mice + DSS (oral administration)	5 mg/kg (oral administration)	-	↓ TNF-α; ↑ TGF-β; ↓ immune cell infiltration and tissue damage	[71]
Pseudoguaianolides		In vitro	Jurkat T cells + TNF-α	5–200 μM	↓ NF-κB	↓ NF-κB DNA-binding	[72]
		In vitro	Jurkat T cells + TNF-α	10 μM	↓ NF-κB	↓ NF-κB DNA-binding and nuclear translocation	[73]
	Helenalin (22)	In vitro	Jurkat CD4$^+$ T-cells	0.5–5 μM	↓ NFAT ↓ NF-κB	↓ IL-2 ↓ proliferation of CD4$^+$ cells	[23][74]
		In vitro	THP-1 cells + LPS	0.52–1.08 μM	↓ NF-κB	↓ IL-1α, IL-19, MCP-3, GM-CSF	[75]
		In vitro	A2780 human ovarian cancer cell line	0.5–2 μM	↓ NF-κB	↓ NF-κB p65 expression	[76]
	11α,13-dihydrohelenalin (23)	In vitro	PBMCs + LPS	2–20 μM	↓ NF-κB and NFAT	↓ IL-2, IL-6, GM-CSF, TNF-α, INF-γ, iNOS	[77]
			Jurkat T-cells + LPS			↓ NF-κB and NFAT levels	
	11α,13-dihydrohelenalin–acetate (24)	In vitro	PBMCs + LPS	2–20 μM	↓ NF-κB and NFAT	↓ IL-2, IL-6, GM-CSF, TNF-α, INF-γ, iNOS	
			Jurkat T-cells + LPS			↓ NF-κB and NFAT levels	
		In vitro	Human granulocytes +	1–600 μM	↓ Arachidonic Acid	↓ Leukotriene C_4 synthase;	[78]

31. Wong, H.; Menendez, I.Y. Sesquiterpene Lactones Inhibit Inducible Nitric Oxide Synthase Gene Expression in Cultured Rat Aortic Smooth Muscle Cells. Biochem. Biophys. Res. Commun. 1999, 262, 375–380.
32. Magni, P.; Ruscica, M.; Dozio, E.; Rizzi, E.; Beretta, G.; Facino, R.M. Parthenolide Inhibits the LPS-induced Secretion of IL-6 and TNF-α and NF-κB Nuclear Translocation in BV-2 Microglia. Phytother. Res. 2012, 26, 1405–1409.
33. Rummel, C.; Gerstberger, R.; Roth, J.; Hübschle, T. Parthenolide attenuates LPS-induced fever, circulating cytokines and markers of brain inflammation in rats. Cytokine 2011, 56, 739–748.

SL Subclass	Compound Name (ID Number)	Model		Compound Concentration Ranges Tested	Inflammatory Pathways	Consequences	References
			Ionophore A23187			↓ 5-lipooxygenase	
Endoperoxide SL	Artemisinin (25)	In vitro	HUVECs + TNF-α	50–200 μM	↓ NF-κB; ↓ MAPKs	↓ ICAM-1, VCAM-1; ↓ adhesion of monocytes	[80]
	Dihydroartemisinin (26)	In vitro	RAW 264.7 macrophages + PMA	5–25 μM	↓ NF-κB, AP-1 and MAPKs	↓ COX-2	[81]

36. Li, S.; Gao, X.; Wu, X.; Cheng, L.; Zhu, L.; Shen, D.; Tong, X. Parthenolide inhibits LPS-induced inflammatory cytokines through the toll-like receptor 4 signal pathway in THP-1 cells. Acta Biochim. Biophys. Sin. 2015, 47, 368–375.
37. Feltenstein, M.; Schühly, W.; Warnick, J.; Fischer, N.; Sufka, K. Anti-inflammatory and anti-hyperalgesic effects of sesquiterpene lactones from Magnolia and Bear's foot. Pharmacol. Biochem. Behav. 2004, 79, 299–302.
38. Pae, H.-O.; Jeong, G.-S.; Woo, W.H.; Rhew, H.Y.; Kim, H.S.; Sohn, D.H.; Kim, Y.-C.; Chung, H.-T. Costunolide inhibits production of tumor necrosis factor-α and interleukin-6 by inducing heme oxygenase-1 in RAW264.7 macrophages. Inflamm. Res. 2007, 56, 520–526.
39. Sobota, R.; Szwed, M.; Kasza, A.; Bugno, M.; Kordula, T. Parthenolide Inhibits Activation of Signal Transducers and Activators of Transcription (STATs) Induced by Cytokines of the IL-6 Family. Biochem. Biophys. Res. Commun. 2000, 267, 329–333.
40. Butturini, E.; Cavalieri, E.; De Prati, A.C.; Darra, E.; Rigo, A.; Shoji, K.; Murayama, N.; Yamazaki, H.; Watanabe, Y.; Suzuki, H.; et al. Two Naturally Occurring Terpenes, Dehydrocostuslactone and Costunolide, Decrease Intracellular GSH Content and Inhibit STAT3 Activation. PLoS ONE 2011, 6, e20174.
41. Scarponi, C.; Butturini, E.; Sestito, R.; Madonna, S.; Cavani, A.; Mariotto, S.; Albanesi, C. Inhibition of Inflammatory and Proliferative Responses of Human Keratinocytes Exposed to the Sesquiterpene Lactones Dehydrocostuslactone and Costunolide. PLoS ONE 2014, 9, e107904.
42. Kang, J.S.; Yoon, Y.D.; Lee, K.H.; Park, S.-K.; Kim, H.M. Costunolide inhibits interleukin-1β expression by down-regulation of AP-1 and MAPK activity in LPS-stimulated RAW 264.7 cells. Biochem. Biophys. Res. Commun. 2004, 313, 171–177.
43. He, Y.; Moqbel, S.A.A.; Xu, L.; Ran, J.; Ma, C.; Xu, K.; Bao, J.; Jiang, L.; Chen, W.; Xiong, Y.; et al. Costunolide inhibits matrix metalloproteinases expression and osteoarthritis via the NF-κB and Wnt/β-catenin signaling pathways. Mol. Med. Rep. 2019, 20, 312–322.
44. Saraswati, S.; Alhaider, A.A.; Abdelgadir, A.M. Costunolide suppresses an inflammatory angiogenic response in a subcutaneous murine sponge model. APMIS 2018, 126, 257–266.
45. Lee, J.; Tae, N.; Lee, J.J.; Kim, T.; Lee, J.-H. Eupatolide inhibits lipopolysaccharide-induced COX-2 and iNOS expression in RAW264.7 cells by inducing proteasomal degradation of TRAF6. Eur. J.

Pharmacol. 2010, 636, 173–180.

46. Formisano, C.; Sanna, C.; Ballero, M.; Chianese, G.; Sirignano, C.; Rigano, D.; Millán, E.; Muñoz, E.; Taglialatela-Scafati, O. Anti-inflammatory sesquiterpene lactones from Onopordum illyricum L. (Asteraceae), an Italian medicinal plant. Fitoterapia 2017, 116, 61–65.
47. Pan, L.; Hu, L.; Zhang, L.; Xu, H.; Chen, Y.; Bian, Q.; Zhu, A.; Wu, H. Deoxyelephantopin decreases the release of inflammatory cytokines in macrophage associated with attenuation of aerobic glycolysis via modulation of PKM2. Int. Immunopharmacol. 2020, 79, 106048.
48. Huang, C.-C.; Lin, K.-J.; Cheng, Y.-W.; Hsu, C.-A.; Yang, S.-S.; Shyur, L.-F. Hepatoprotective effect and mechanistic insights of deoxyelephantopin, a phyto-sesquiterpene lactone, against fulminant hepatitis. J. Nutr. Biochem. 2013, 24, 516–530.
49. Benteldjoune, M.; Chini, M.G.; Iannuzzi, A.M.; Kabouche, A.; Kabouche, Z.; D'ambola, M.; Marzocco, S.; Autore, G.; Bifulco, G.; De Tommasi, N. Guaianolides from Ormenis mixta: Structural Insights and Evaluation of Their Anti-inflammatory Profile. Planta Med. 2019, 85, 947–956.
50. Zhou, Q.; Zhang, W.-X.; He, Z.-Q.; Wu, B.-S.; Shen, Z.-F.; Shang, H.-T.; Chen, T.; Wang, Q.; Chen, Y.-G.; Han, S.-T. The Possible Anti-Inflammatory Effect of Dehydrocostus Lactone on DSS-Induced Colitis in Mice. Evid. Based Complement. Altern. Med. 2020, 2020, 1–8.
51. Kim, S.Y.; Heo, S.; Kim, S.H.; Kwon, M.; Sung, N.J.; Ryu, A.-R.; Lee, M.-Y.; Park, S.-A.; Youn, H.-S. Suppressive effects of dehydrocostus lactone on the toll-like receptor signaling pathways. Int. Immunopharmacol. 2020, 78, 106075.
52. Sun, Z.; Li, G.; Tong, T.; Chen, J. Micheliolide suppresses LPS-induced neuroinflammatory responses. PLoS ONE 2017, 12, e0186592.
53. Viennois, E.; Xiao, B.; Ayyadurai, S.; Wang, L.; Wang, P.G.; Zhang, Q.; Chen, Y.; Merlin, D. Micheliolide, a new sesquiterpene lactone that inhibits intestinal inflammation and colitis-associated cancer. Lab. Investig. 2014, 94, 950–965.
54. Qin, X.; Jiang, X.; Wang, Y.; Miao, Z.; He, W.; Yang, G.; Lv, Z.; Yu, Y.; Zheng, Y. Micheliolide inhibits LPS-induced inflammatory response and protects mice from LPS challenge. Sci. Rep. 2016, 6, 23240.
55. Xu, H.; Wang, J.; Wang, C.; Chang, G.; Lin, Y.; Zhang, H.; Zhang, H.; Li, Q.; Pang, T. Therapeutic effects of micheliolide on a murine model of rheumatoid arthritis. Mol. Med. Rep. 2014, 11, 489–493.
56. Cho, J.Y.; Baik, K.U.; Jung, J.H.; Park, M.H. In vitro anti-inflammatory effects of cynaropicrin, a sesquiterpene lactone, from Saussurea lappa. Eur. J. Pharmacol. 2000, 398, 399–407.

57. Abderrazak, A.; Couchie, D.; Mahmood, D.; El Hage, R.; Vindis, C.; Laffargue, M.; Mateo, V.; Buechele, B.; Ayala, M.R.; El Gaafary, M.; et al. Anti-Inflammatory and Antiatherogenic Effects of the NLRP3 Inflammasome Inhibitor Arglabin in ApoE2.Ki Mice Fed a High-Fat Diet. Circulation 2015, 131, 1061–1070.

58. Matos, M.S.; Anastácio, J.D.; Allwood, J.W.; Carregosa, D.; Marques, D.; Sungurtas, J.; McDougall, G.J.; Menezes, R.; Matias, A.A.; Stewart, D.; et al. Assessing the Intestinal Permeability and Anti-Inflammatory Potential of Sesquiterpene Lactones from Chicory. Nutrients 2020, 12, 3547.

59. Cavin, C.; Delannoy, M.; Malnoe, A.; Debefve, E.; Touché, A.; Courtois, D.; Schilter, B. Inhibition of the expression and activity of cyclooxygenase-2 by chicory extract. Biochem. Biophys. Res. Commun. 2005, 327, 742–749.

60. Chun, J.; Choi, R.J.; Khan, S.; Lee, D.-S.; Kim, Y.-C.; Nam, Y.-J.; Kim, Y.S. Alantolactone suppresses inducible nitric oxide synthase and cyclooxygenase-2 expression by down-regulating NF-κB, MAPK and AP-1 via the MyD88 signaling pathway in LPS-activated RAW 264.7 cells. Int. Immunopharmacol. 2012, 14, 375–383.

61. Ren, Y.; Yue, B.; Ren, G.; Yu, Z.; Luo, X.; Sun, A.; Zhang, J.; Han, M.; Wang, Z.; Dou, W. Activation of PXR by alantolactone ameliorates DSS-induced experimental colitis via suppressing NF-κB signaling pathway. Sci. Rep. 2019, 9, 16636.

62. Liu, L.; Hua, Y.; Wang, D.; Shan, L.; Zhang, Y.; Zhu, J.; Jin, H.; Li, H.; Hu, Z.; Zhang, W. A Sesquiterpene Lactone from a Medicinal Herb Inhibits Proinflammatory Activity of TNF-α by Inhibiting Ubiquitin-Conjugating Enzyme UbcH5. Chem. Biol. 2014, 21, 1341–1350.

63. Wang, X.; Tang, S.-A.; Wang, R.; Qiu, Y.; Jin, M.; Kong, D. Inhibitory Effects of JEUD-38, a New Sesquiterpene Lactone from Inula japonica Thunb, on LPS-Induced iNOS Expression in RAW264.7 Cells. Inflammation 2015, 38, 941–948.

64. Fonseca, L.C.; Dadarkar, S.S.; Lobo, A.S.; Mishra, P.B.; Thakkar, A.D.; Chandrababu, S.; Padigaru, M. NF-κB-mediated anti-inflammatory activity of the sesquiterpene lactone 7-hydroxyfrullanolide. Eur. J. Pharmacol. 2011, 657, 41–50.

65. Fonseca, L.C.; Dadarkar, S.S.; Lobo, A.S.; Suthar, A.C.; Chauhan, V.S.; Chandrababu, S.; Sharma, S.D.; Dagia, N.M.; Padigaru, M. 7-hydroxyfrullanolide, a sesquiterpene lactone, inhibits pro-inflammatory cytokine production from immune cells and is orally efficacious in animal models of inflammation. Eur. J. Pharmacol. 2010, 644, 220–229.

66. Choi, H.-G.; Lee, D.-S.; Li, B.; Choi, Y.H.; Lee, S.-H.; Kim, Y.-C. Santamarin, a sesquiterpene lactone isolated from Saussurea lappa, represses LPS-induced inflammatory responses via expression of heme oxygenase-1 in murine macrophage cells. Int. Immunopharmacol. 2012, 13, 271–279.

67. Ferrari, F.C.; Ferreira, L.C.; Souza, M.R.; Paula, C.A.; Rezende, S.A.; Grabe-Guimarães, A.; Saúde-Guimarães, D. Anti-Inflammatory Sesquiterpene Lactones from Lychnophora trichocarpha Spreng. (Brazilian Arnica). Phytother. Res. 2012, 27, 384–389.

68. Zarpelon, A.C.; Fattori, V.; Souto, F.O.; Pinto, L.G.; Pinho-Ribeiro, F.A.; Ruiz-Miyazawa, K.W.; Turato, W.M.; Cunha, T.M.; Da Costa, F.B.; Cunha, F.Q.; et al. The Sesquiterpene Lactone, Budlein A, Inhibits Antigen-Induced Arthritis in Mice: Role of NF-κB and Cytokines. Inflammation 2017, 40, 2020–2032.

69. Valério, D.A.; Cunha, T.M.; Arakawa, N.S.; Lemos, H.D.P.; Da Costa, F.B.; Parada, C.A.; Ferreira, S.H.; Cunha, F.Q.; Verri, W.A. Anti-inflammatory and analgesic effects of the sesquiterpene lactone budlein A in mice: Inhibition of cytokine production-dependent mechanism. Eur. J. Pharmacol. 2007, 562, 155–163.

70. Fattori, V.; Zarpelon, A.C.; Staurengo-Ferrari, L.; Borghi, S.M.; Zaninelli, T.H.; Da Costa, F.B.; Alves-Filho, J.C.; Cunha, T.M.; Cunha, F.Q.; Casagrande, R.; et al. Budlein A, a Sesquiterpene Lactone from Viguiera robusta, Alleviates Pain and Inflammation in a Model of Acute Gout Arthritis in Mice. Front. Pharmacol. 2018, 9, 1076.

71. Sabel, R.; Fronza, A.; Carrenho, L.; Maes, A.; Barros, M.; Pollo, L.A.E.; Biavatti, M.; D'Herde, K.; Vandenabeele, P.; Kreuger, M. Anti-inflammatory activity of the sesquiterpene lactone diacethylpiptocarphol in dextransulfate sodium-induced colitis in mice. J. Ethnopharmacol. 2019, 245, 112186.

72. Lyss, G.; Schmidt, T.J.; Merfort, I.; Pahl, H.L. Helenalin, an Anti-Inflammatory Sesquiterpene Lactone from Arnica, Selectively Inhibits Transcription Factor NF-κB. Biol. Chem. 1997, 378, 951–962.

73. Lyß, G.; Knorre, A.; Schmidt, T.J.; Pahl, H.L.; Merfort, I. The Anti-inflammatory Sesquiterpene Lactone Helenalin Inhibits the Transcription Factor NF-κB by Directly Targeting p65. J. Biol. Chem. 1998, 273, 33508–33516.

74. Berges, C.; Fuchs, D.; Opelz, G.; Daniel, V.; Naujokat, C. Helenalin suppresses essential immune functions of activated CD4+ T cells by multiple mechanisms. Mol. Immunol. 2009, 46, 2892–2901.

75. Zwicker, P.; Schultze, N.; Niehs, S.; Albrecht, D.; Methling, K.; Wurster, M.; Wachlin, G.; Lalk, M.; Lindequist, U.; Haertel, B. Differential effects of Helenalin, an anti-inflammatory sesquiterpene lactone, on the proteome, metabolome and the oxidative stress response in several immune cell types. Toxicol. Vitr. 2017, 40, 45–54.

76. Lim, C.B.; Fu, P.Y.; Ky, N.; Zhu, H.S.; Feng, X.; Li, J.; Srinivasan, K.G.; Hamza, M.S.; Zhao, Y. NF-κB p65 repression by the sesquiterpene lactone, Helenalin, contributes to the induction of autophagy cell death. BMC Complement. Altern. Med. 2012, 12, 93.

77. Gertsch, J.; Sticher, O.; Schmidt, T.; Heilmann, J. Influence of helenanolide-type sesquiterpene lactones on gene transcription profiles in Jurkat T cells and human peripheral blood cells: Anti-inflammatory and cytotoxic effects. Biochem. Pharmacol. 2003, 66, 2141–2153.
78. Tornhamre, S.; Schmidt, T.J.; Näsman-Glaser, B.; Ericsson, I.; Lindgren, J. Åke Inhibitory effects of helenalin and related compounds on 5-lipoxygenase and leukotriene C4 synthase in human blood cells. Biochem. Pharmacol. 2001, 62, 903–911.
79. Wu, Z.-L.; Wang, J.-X.; Chen, L.-P.; Dong, H.-Y.; Li, H.-L.; Zhang, W.-D. Five rare C 32 sesquiterpene lactone dimers with anti-inflammation activity from Vladimiria souliei. Fitoterapia 2018, 125, 117–122.
80. Wang, Y.; Cao, J.; Zhaofang, Y.; Xie, Y.; Xu, Z.; Yin, Z.; Gao, L.; Wang, C. Artemisinin inhibits monocyte adhesion to HUVECs through the NF-κB and MAPK pathways in vitro. Int. J. Mol. Med. 2016, 37, 1567–1575.
81. Kim, H.G.; Yang, J.H.; Han, E.H.; Choi, J.H.; Khanal, T.; Jeong, M.H.; Jeong, T.C.; Jeong, H.G. Inhibitory effect of dihydroartemisinin against phorbol ester-induced cyclooxygenase-2 expression in macrophages. Food Chem. Toxicol. 2013, 56, 93–99.
82. Siedle, B.; Cisielski, S.; Murillo, R.; Löser, B.; Castro, V.; Klaas, C.; Hucke, O.; Labahn, A.; Melzig, M.; Merfort, I. Sesquiterpene lactones as inhibitors of human neutrophil elastase. Bioorg. Med. Chem. 2002, 10, 2855–2861.